Title

3,4-diaminobenzoic acid derivatives as inhibitors of the oxytocinase subfamily of M1 aminopeptidases with immune-regulating properties.

Journal

Journal of medicinal chemistry, 58(3)

ISSN

0022-2623

Authors

Papakyriakou, Athanasios
Zervoudi, Efthalia
Tsoukalidou, Sofia
et al.

Publication Date

2015-02-01

DOI

10.1021/jm501867s

Peer reviewed

Journal of Medicinal Chemistry

Article

pubs.acs.org/jmc

3,4-Diaminobenzoic Acid Derivatives as Inhibitors of the Oxytocinase Subfamily of M1 Aminopeptidases with Immune-Regulating Properties

Athanasios Papakyriakou,[†,‡] Efthalia Zervoudi,[†] Sofia Tsoukalidou,[†] Francois-Xavier Mauvais,[§] Georgia Sfyroera,[†] Dimitrios C. Mastellos,[†] Peter van Endert,[§] Emmanuel A. Theodorakis,[‡] Dionisios Vourloumis,*[,†] and Efstratios Stratikos*[,†]

[†]National Center for Scientific Research "Demokritos", Aghia Paraskevi, 15310 Athens, Greece

[‡]Department of Chemistry and Biochemistry, University of California−San Diego, 9500 Gilman Drive, San Diego, California 92093-0358, United States

[§]Institut National de la Santé et de la Recherche Médicale, Unité 1151; Université Paris Descartes, Sorbonne Paris Cité; Centre National de la Recherche Scientifique, Unité 8253, 75015 Paris, France

Supporting Information

ABSTRACT: Members of the oxytocinase subfamily of M1 aminopeptidases (ERAP1, ERAP2, and IRAP) play important roles in both the adaptive and innate human immune responses. Their enzymatic activity can contribute to the pathogenesis of several major human diseases ranging from viral and parasitic infections to autoimmunity and cancer. We have previously demonstrated that diaminobenzoic acid derivatives show promise as selective inhibitors for this group of aminopeptidases. In this study, we have thoroughly explored a series of 3,4-diaminobenzoic acid derivatives as inhibitors of this class of enzymes, achieving submicromolar inhibitors for ERAP2 (IC_{50} = 237 nM) and IRAP (IC_{50} = 105 nM). Cell-based analysis indicated that the lead compounds can be effective in downregulating macrophage activation induced by lipopolysaccharide and interferon-γ as well as cross-presentation by bone marrow-derived dendritic cells. Our results indicate that this class of inhibitors may be useful for the targeted downregulation of immune responses.

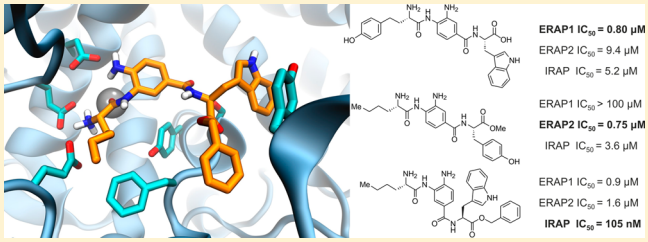

INTRODUCTION

The three members of the oxytocinase subfamily of M1 aminopeptidases,[1] namely, endoplasmic reticulum aminopeptidases 1 and 2 (ERAP1 and ERAP2) and insulin regulated aminopeptidase (IRAP), henceforth referred to as antigen processing aminopeptidases (APAs), have been, during recent years, shown to have important biological functions, primarily in the regulation of human adaptive and innate immune responses. ERAP1 and ERAP2 act in intracellular antigen processing and are responsible not only for the correct generation of many antigenic epitopes but also for the destruction of others.[2−4] By this function, these enzymes can regulate cellular immune responses to infected or diseased cells and contribute to immune evasion by pathogens and cancer cells as well as to autoimmunity.[5] IRAP combines the specificity of ERAP1 and ERAP2 and functions in a specialized pathway of antigen processing and presentation called cross-presentation, present in dendritic cells (DCs), possibly regulating early stages of inflammatory immune responses.[6,7] ERAP1 and ERAP2 are polymorphic, and several coding single nucleotide polymorphisms in these genes have been associated with predisposition to major human diseases, ranging from viral and parasitic infections to cancer and inflammatory diseases with autoimmune etiology (reviewed in refs 8 and 9). Recently, a secreted form of ERAP1 has also been implicated in innate immunity responses: macrophages activated by interferon-gamma and liposaccharides secrete ERAP1 in a TLR-dependent pathway,[10,11] resulting in the enhancement of their phagocytic activity and inflammatory potential. Similarly, ERAP1 knockout mice show increased activation of NK and NKT cells,[12] consistent with a role of ERAP1 in regulating both adaptive and innate immune responses. ERAP1 polymorphic variation was recently shown to quantitatively affect innate immune responses.[13] Since natural polymorphic variation of ERAP1 and ERAP2 can generate a range of enzymatic activities in the population, it has been hypothesized that the activity of these enzymes is an important regulator of immune responses in humans.[14]

Inhibition of APAs is a promising approach for selectively regulating immune responses. ERAP1 knockout mice present a distinct repertoire of antigenic peptides on their cell sur-

Received: December 3, 2014
Published: January 18, 2015

DOI: 10.1021/jm501867s
J. Med. Chem. 2015, 58, 1524−1543

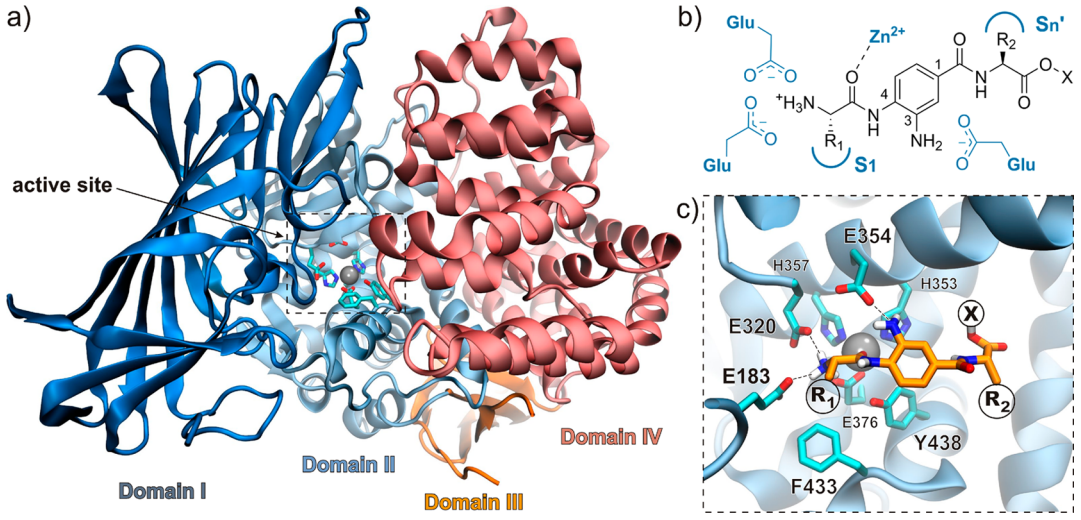

Figure 1. (a) Crystallographic structure of ERAP1 in the closed conformation (PDB ID: 2YD0), illustrating the domain organization and the active site of the enzyme. The catalytic zinc is shown as a gray sphere, and protein residues are shown as sticks with carbon in cyan, nitrogen in blue, oxygen in red, and sulfur in yellow. (b) Schematic representation of the 1,4-disubstituted DABA inhibitors, where R_1 and R_2 are L-α-amino acid side chains targeting the S1 and Sn′ subsites of the aminopeptidases, respectively, and X = H, Me, or Bn. (c) Molecular model of the 1,4-disubstituted DABA scaffold (carbon atoms shown in orange) docked at the active site of ERAP1. The α-amino terminal docking residues are E183 and E320; the zinc-binding residues are H353, H357, and E376, whereas the catalytic E354 is expected to interact with the free aniline of the inhibitors. Catalytically important Y438 and conserved F433 that forms the bottom of S1 are also shown.

face.[15−17] Genetic downregulation of ERAP1 can lead to novel cellular immune responses, including nonclassical cellular responses, through the activation of cytotoxic-T lymphocytes and natural killer cells.[18−20] A pseudophosphinic peptide APA inhibitor has been demonstrated recently to enhance antigen presentation and elicit potent anti-cancer CTL responses toward a cryptic antigenic epitope that is normally destroyed by ERAP1.[21] On the other hand, downregulation of ERAP1 has been recently shown to reduce CTL responses against a viral epitope associated with the pathogenesis of autoimmunity.[22] As a result, the pharmacological regulation of APA activity has attracted significant scientific interest over the past few years as a promising area with therapeutic potential. Unfortunately, most characterized APA inhibitors suffer either from low potency or low selectivity, necessitating the exploration of other approaches. Selectively targeting only one of the members of this family of aminopeptidases may be highly desirable in order to fine-tune immune responses while minimizing potential side effects.

We recently demonstrated that using 3,4-diaminobenzoic acid (DABA) as a scaffold is a valid approach for generating inhibitors for this class of aminopeptidases with promising selectivity profiles.[23] In this study, we explored the DABA derivatives more extensively, with the aim of improving their potency and selectivity toward ERAP1, ERAP2, and IRAP. By employing a rational, structure-based optimization procedure, we identified potent inhibitors for ERAP2 (237 nM) and IRAP (105 nM) as well as a highly selective ERAP2 inhibitor (755 nM) in comparison to ERAP1 (>100 μM).

To evaluate the biological potential of the discovered inhibitors, we utilized two specialized cellular assays relevant to innate and adaptive inflammatory immune responses. The low-micromolar ERAP1 inhibitor, **4a** (2 μM), was able to inhibit macrophage activation by inflammatory mediators with submicromolar potency. The most potent IRAP inhibitor, **4u**, was able to block the IRAP-dependent cross-presentation pathway in dendritic cells with low-nanomolar potency. These results suggest that these compounds may hold promise upon further development as targeted modulators of inflammatory immune responses.

RESULTS AND DISCUSSION

Inhibitor Design. Selection of the amino acid side chains used for inhibitor design was based on a previous study on the selectivity profile of the S1 subsite of ERAP1, ERAP2, and IRAP using a library of 82 fluorogenic substrates.[24] Specifically, it was suggested that ERAP1 displays a general preference for substrates comprising long, aromatic or hydrophobic, R_1 side chains (Figure 1). In contrast, the S1 subsite of ERAP2 exhibits higher selectivity for positively charged groups, especially Arg and homo-Arg, whereas IRAP combines the specificity of ERAP1 and ERAP2. All D-amino acid-based substrates were poorly processed by the three enzymes, suggesting that the L configuration is a prerequisite for binding. In our initial efforts,[23] we utilized homo-Phe (hPhe), which is predicted to be ideally accommodated within the S1 specificity pocket of ERAP1 due to π-stacking interactions with a conserved aromatic residue (F433/450/544 for ERAP1/ERAP2/IRAP, respectively). In combination with the positively charged side chain of Lys for R_2, 1,3-substituted derivative **4a** displayed low-micromolar affinity for ERAP1 (IC_{50} = 2.0 ± 0.6 μM) and >10-fold selectivity for ERAP2. In this study, we explored the contribution of hydrophobic (Leu and nor-Leu), aromatic (Phe, Tyr, homo-Tyr(OBn), Ser-OBn), and positively charged Arg side chains at position R_1, while keeping lysine in the R_2 position (Figure 1). Subsequently, a series of 1,3-substituted DABA derivatives was synthesized by combining the above-mentioned R_1 amino acids with hydrophobic (Val), polar (Thr), aromatic (Tyr and Trp), and positively charged Arg side chains at position R_2. Our collection of 1,3-disubstituted DABA analogues was enriched with a selection of 1,4-disubstituted DABA to evaluate the different binding orientations of the inhibitors. A subset of monosubstituted DABA derivatives was also evaluated for direct comparison.

DOI: 10.1021/jm501867s
J. Med. Chem. 2015, 58, 1524−1543

Scheme 1. Synthesis of the 1,3- and 1,4-Substituted 3,4-Diaminobenzoic Acid Derivatives[a]

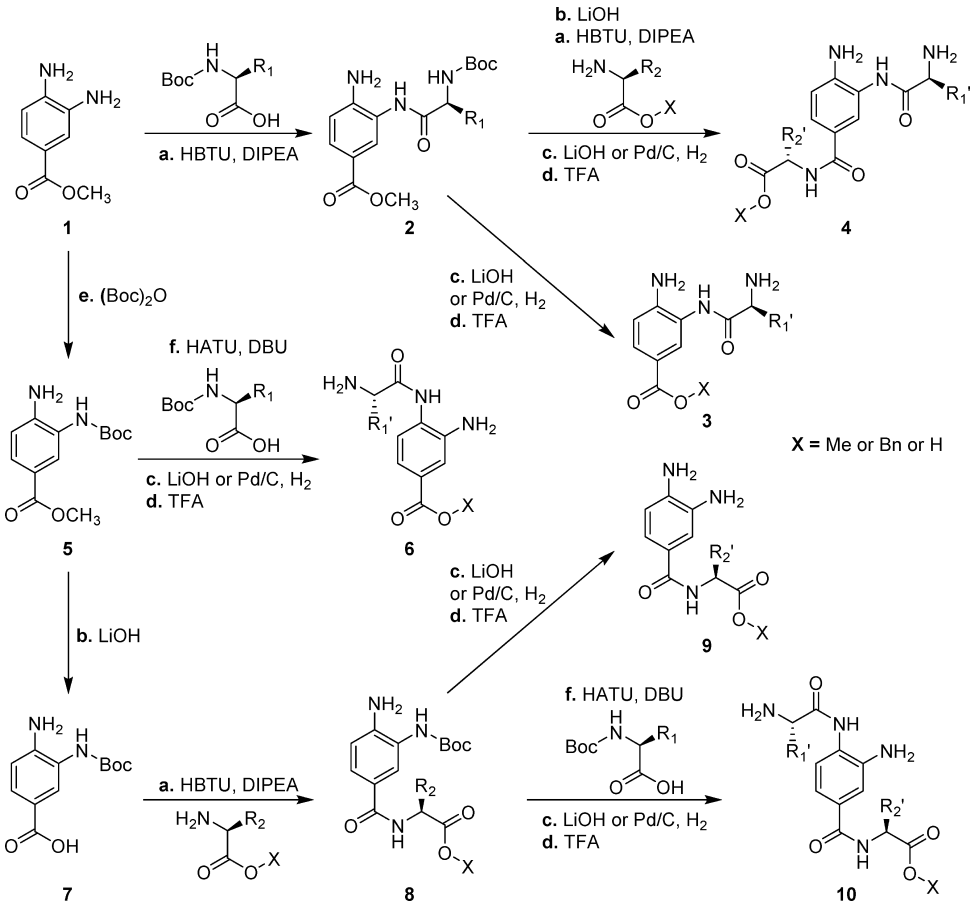

[a]Reagents and conditions: (a) protected amino acid (1.1−1.5 equiv), HBTU (2.0−3.0 equiv), DIEA (3.0−4.0 equiv), DMF, 4−12 h, rt, 65−92%; (b) LiOH 1 M (20 equiv), dioxane/H_2O (1:1), 3−6 h, rt, 87−95%. (c) LiOH 1 M (20 equiv), dioxane/H_2O (1:1), 3−6 h, rt, or cat. Pd/C (10 wt %), H_2, MeOH, 1−2 h, rt, 90−95%. (d) TFA/CH_2Cl_2 (1:2), 20−40 min, rt, 95−98%. (e) $(Boc)_2O$ (1.0 equiv), Gu·HCl (15 mol %), EtOH, 40 min, 45 °C, 78%. (f) Protected amino acid (2.0 equiv), HATU (3.0 equiv), DBU (4.0 equiv), DMF, 24−36 h, rt, 45−72%. R_1: side chain of L-α-amino acid selected from Leu, nor-Leu, Ser(OBn), Phe, homo-Phe, Tyr(OBn), homo-Tyr(OBn), or Arg(Z)$_2$. R_2: side chain of L-α-amino acid selected from Val, Thr, Tyr(O-tBu), Trp, Lys(Boc), ornithine(Boc), or Arg(Z)$_2$. R_1', R_2': the corresponding deprotected L-amino acid side chains. X: H, OMe, or OBn.

Chemistry. General synthetic routes for all new analogues are presented in Scheme 1. As described previously,[23] 1,3-disubstituted DABA derivatives **4** were obtained through the coupling of *N*-Boc-protected amino acids, furnishing intermediates **2**, followed by saponification of the corresponding methyl ester, formation of the second amide bond using *O*-methyl or *O*-benzyl protected amino acids, and global removal of the protecting groups. Following an analogous route, our approach was extended to furnish 1,4-disubstituted DABA derivatives **10** starting from 3-*N*-Boc protected DABA intermediate **7**. In this case, the second amide bond formation at the less reactive 4-NH_2 was achieved in higher yields by utilizing a combination of HATU as the coupling reagent and DBU as the base. As mentioned before, monosubstituted DABA derivatives **3**, **6**, and **9** were also prepared, as presented in Scheme 1, for direct comparison.

In Vitro Evaluation. The inhibitory potency of the synthesized compounds for the three enzymes was determined using an established fluorogenic assay.[23] Regarding monosubstituted DABA derivatives **3a**−**3g′** (Table 1), **6a**−**6f**, and **9a**−**9d** (Table 2), the in vitro evaluation did not reveal any low-micromolar (<10 μM) ERAP1 inhibition. In contrast, 4-amino substituted DABA derivatives **6e** (R_1=Nle) and **6f** (R_1=Arg) displayed IC_{50} values of 1.1 and 2.5 μM for ERAP2, respectively, whereas **6b** (R_1=Tyr(OBn)) exhibits IC_{50} = 1.7 μM for IRAP.

In the effort to optimize our previous hit **4a**, we initially substituted R_2=Lys for the shorter side chain of L-ornithine (Orn). Surprisingly, both the methyl ester and the carboxylic acid of 1,3-hPhe-DABA-Orn derivatives (**4d** and **4d′**, respectively) were found to be inactive (IC_{50} > 100 μM) for all three aminopeptidases (Table 1), indicating a very important interaction associated with the longer Lys side chain. Substitution of hPhe by the shorter Phe side chain yielded compound **4e**, which is inactive for ERAP1, although it is more potent than **4a** for ERAP2 and IRAP, demonstrating the importance of the longer hPhe side chain, as proposed previously.[23] From the remaining 1,3-disubstituted DABA-Lys derivatives, **4e**−**4l**, the in vitro evaluation revealed several moderate inhibitors (IC_{50} = 2−8 μM) for ERAP2 and IRAP only, with most compounds being inactive toward ERAP1 (Table 1).

The next generation of 1,3-disubstituted DABA derivatives, **4m**−**4y**, was designed by combining Tyr, hTyr, Nle, and Arg for R_1 with Val, Tyr, and Trp for R_2 (Table 1). Although Tyr in the R_1 position yielded low-affinity inhibitors (**4m**−**4p′**) for all

DOI: 10.1021/jm501867s
J. Med. Chem. 2015, 58, 1524−1543

Table 1. In Vitro Evaluation of the Designed 1,3-Substituted DABA Derivatives for ERAP1, ERAP2, and IRAP*

ID	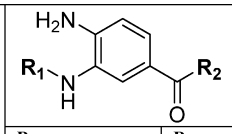		IC_{50} (μM)		
	R_1	R_2	ERAP1	ERAP2	IRAP
3a	NH_2-L-Tyr(OBn)	OMe	*NI*	*NI*	10.0±1.0
3a′	NH_2-L-Tyr(OBn)	OH	*NI*	*NI*	10.7±1.5
3b	NH_2-L-Tyr	OMe	*NI*	>100	57±9.5
3b′	NH_2-L-Tyr	OH	>100	3.2±0.8	10.9±1.9
3c	NH_2-L-hTyr(OBn)	OMe	*NI*	*NI*	2.1±0.4
3d	NH_2-L-hTyr-OMe	OMe	>100	*NI*	12±2.0
3e	NH_2-L-Leu	OMe	*NI*	*NI*	*NI*
3e′	NH_2-L-Leu	OH	*NI*	*NI*	*NI*
3f	NH_2-L-Nle	OMe	>100	9.8±1.0	7.2±1.0
3g	NH_2-L-Arg	OMe	*NI*	3.7±0.5	14.6±2.0
3g′	NH_2-L-Arg	OH	*NI*	>100	34±7.5
4a[α]	NH_2-L-hPhe	L-Lys-OMe	2.0±0.6	24.9±1.2	10.3±0.6
4b[α]	NH_2-L-hPhe	L-Trp-OBn	*NI*	23.9 ± 0.8	1.3±0.1
4c[α]	NH_2-L-hPhe	L-Tyr-OMe	7.7±0.4	>100	3.6±0.4
4d	NH_2-L-hPhe	L-Orn-OMe	*NI*	*NI*	*NI*
4d′	NH_2-L-hPhe	L-Orn-OH	*NI*	*NI*	>100
4e	NH_2-L-Phe	L-Lys-OH	*NI*	2.6±0.3	3.8±0.6
4f	NH_2-L-Tyr	L-Lys-OH	*NI*	4.5±0.4	4.8±0.4
4g	NH_2-L-hTyr	L-Lys-OMe	>100	4.8±0.8	10.7±2.8
4h	NH_2-L-hTyr(OBn)	L-Lys-OMe	>100	13±2.5	5.7±0.5
4i	NH_2-L-Ser(OBn)	L-Lys-OMe	*NI*	*NI*	*NI*
4j	NH_2-L-Leu	L-Lys-OMe	*NI*	52±13	*NI*
4j′	NH_2-L-Leu	L-Lys-OH	6.8±1.1	2.1±0.2	4.1±0.8
4k	NH_2-L-Nle	L-Lys-OMe	18.3±0.3	8.3±1.5	>100
4l	NH_2-L-Arg	L-Lys-OMe	42±8	17±3	*NI*
4m	NH_2-L-Tyr	L-Val-OBn	*NI*	50±14	12±1.0
4m′	NH_2-L-Tyr	L-Val-OH	*NI*	>100	>100
4n	NH_2-L-Tyr	L-Tyr-OMe	110±50	33±6.5	22±4.5
4o	NH_2-L-Tyr	L-Thr-OMe	>100	39±9.5	>100
4p	NH_2-L-Tyr	L-Trp-OBn	9.8±0.8	40±14.5	7.1±1.2
4p′	NH_2-L-Tyr	L-Trp-OH	12.1±1.0	>100	>100
4q	NH_2-L-hTyr(OBn)	L-Trp-OBn	>100	>100	0.933±0.14
4r	NH_2-L-hTyr	L-Trp-OH	38.4±9.5	>100	4.4±0.7
4s	NH_2-L-Nle	L-Val-OBn	>100	>100	1.3±0.4
4s′	NH_2-L-Nle	L-Val-OH	*NI*	>100	>100
4t	NH_2-L-Nle	L-Tyr-OMe	>100	6.4±0.4	1.2±0.4
4u	NH_2-L-Nle	L-Trp-OBn	0.92±0.20	1.6±0.3	0.105±0.063
4u′	NH_2-L-Nle	L-Trp-OH	3.6±0.6	3.8±0.3	0.296±0.090
4v	NH_2-L-Nle	L-Arg-OMe	10.7±2.1	2.5±0.3	31±7.5
4w	NH_2-L-Arg	L-Val-OH	*NI*	5.0±1.0	3.3±0.6
4x	NH_2-L-Arg	L-Tyr-OMe	9.6±0.2	0.518±0.043	0.966±0.050
4y	NH_2-L-Arg	L-Trp-OH	1.2±0.2	0.589±0.109	0.655±0.040

*NI, no inhibition observed up to 100 μM; >100 indicates that a limited inhibition is observed in the 50−100 μM range. [α]Data taken from ref 23.

three enzymes, hTyr in combination with Trp displayed low-micromolar inhibition for IRAP (**4q** and **4r**). In particular, **4q** proved to be the most selective IRAP inhibitor against both ERAP1 and ERAP2 (IC_{50} > 100 μM). The combination of R_1═Nle (**4s**−**4v**) or Arg (**4w**−**4y**) with R_2═Tyr or Trp provided the most potent inhibitors. Compound **4u** is the most potent inhibitor of ERAP1 (IC_{50} = 0.92 μM) and IRAP (IC_{50} = 105 nM), followed by its corresponding carboxylic acid **4u′** (IC_{50} = 296 nM for IRAP). It is interesting to note that **4s** and **4t** are both significantly selective inhibitors of IRAP (IC_{50} = 1.2−1.3 μM) with respect to ERAP1 (IC_{50} > 100 μM). As predicted, Arg in the R_1 position provided two more submicromolar inhibitors, **4x** and **4y**, for both ERAP2 and IRAP, with **4x** (IC_{50} = 518 nM) displaying a ∼20-fold selectivity with respect to ERAP1 (IC_{50} = 9.6 μM).

Concerning the in vitro evaluation of the 1,4-disubstituted DABA derivatives (Table 2), our results indicate a significant structural effect from the orientation of the two amino acid substituents on their inhibitory effect, especially regarding ERAP1. A striking example is inactive compound **10a**, which is the regioisomer of the initial ERAP1 hit, **4a** (IC_{50} = 2.0 μM). In

Table 2. In Vitro Evaluation of the Designed 1,4-Substituted DABA Derivatives for ERAP1, ERAP2, and IRAP*

ID	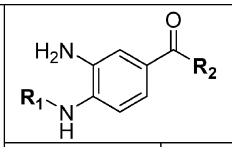		IC_{50} (μM)		
	R_1	R_2	ERAP1	ERAP2	IRAP
6a	NH_2-L-hPhe	OMe	>100	58±18	31±4.0
6b	NH_2-L-Tyr(OBn)	OMe	*NI*	*NI*	1.7±0.2
6c	NH_2-L-Tyr	OMe	*NI*	58±12	8.3±1.0
6d	NH_2-L-Leu	OMe	*NI*	>100	*NI*
6e	NH_2-L-Nle	OMe	*NI*	1.1±0.2	3.3±0.5
6f	NH_2-L-Arg	OMe	*NI*	2.5±0.7	39.6±2.1
9a	H	L-Lys-OMe	>100	*NI*	>100
9b	H	L-Tyr-OMe	*NI*	*NI*	9.9±2.7
9c	H	L-Trp-OBn	*NI*	>100	22.5±2.5
9c′	H	L-Trp-OH	>100	1.9±0.3	>100
9d	H	L-Arg-OMe	35±10	*NI*	2.5±0.9
10a	NH_2-L-hPhe	L-Lys-OMe	*NI*	*NI*	20.6±4.0
10b	NH_2-L-hPhe	L-Val-OBn	*NI*	>100	14.4±3.0
10b′	NH_2-L-hPhe	L-Val-OH	*NI*	>100	20.2±2.5
10c	NH_2-L-hPhe	L-Tyr-OMe	9.4±0.7	5.5±0.6	1.3±0.2
10d	NH_2-L-hPhe	L-Trp-OBn	13.4±3.0	11±2.5	2.4±0.6
10e	NH_2-L-hPhe	L-Arg-OMe	12±1.3	11.8±1.5	4.7±0.6
10f	NH_2-L-Tyr(OBn)	L-Tyr-OMe	*NI*	16±4.5	2.9±0.4
10g	NH_2-L-Tyr	L-Tyr-OMe	16.7±1.5	15.1±2.5	3.7±0.5
10h	NH_2-L-Tyr(OBn)	L-Trp-OBn	1.1±0.3	20.5±2.0	3.8±0.7
10h′	NH_2-L-Tyr	L-Trp-OH	19.5±4.0	4.8±0.8	1.3±0.2
10i	NH_2-L-Tyr	L-Lys-OMe	>100	>100	70±19
10j	NH_2-L-hTyr(OBn)	L-Trp-OBn	*NI*	70±10	3.4±0.5
10j′	NH_2-L-hTyr	L-Trp-OH	0.80±0.16	9.4±1.6	5.2±0.6
10k	NH_2-L-Leu	L-Trp-OBn	8.9±1.5	21±4.5	3.7±0.9
10l	NH_2-L-Leu	L-Lys-OMe	*NI*	*NI*	>100
10m	NH_2-L-Nle	L-Val-OBn	>100	6.2±1.9	3.9±1.0
10m′	NH_2-L-Nle	L-Val-OH	*NI*	38±12	>100
10n	NH_2-L-Nle	L-Tyr-OMe	>100	0.755±0.100	3.6±0.7
10o	NH_2-L-Nle	L-Trp-OBn	2.5±0.5	0.709±0.050	0.438±0.010
10o′	NH_2-L-Nle	L-Trp-OH	2.8±0.5	0.237±0.030	1.7±0.4
10p	NH_2-L-Nle	L-Lys-OMe	*NI*	30.6±12	35.7±12.5
10q	NH_2-L-Arg	L-Tyr-OMe	2.6±0.3	1.4±0.4	2.2±0.2
10r	NH_2-L-Arg	L-Trp-OH	38.2±9.5	1.1±0.1	7.6±0.6
10s	NH_2-L-Arg	L-Lys-OMe	*NI*	11.8±1.0	4.9±0.6

*NI, no inhibition observed up to 100 μM; >100 indicates that a limited inhibition is observed in the 50−100 μM range.

contrast, the inhibitory effect of low-micromolar IRAP inhibitors **4b** (IC_{50} = 1.3 μM) and **4c** (IC_{50} = 2.8 μM) is marginally affected at their corresponding para-isomers **10d** (IC_{50} = 2.4 μM) and **10c** (IC_{50} = 1.3 μM), respectively.

By employing Tyr in the R_1 position, we obtained two more potent inhibitors, **10h**, with IC_{50} = 1.1 μM for ERAP1, and **10h′**, with IC_{50} = 1.3 μM for IRAP. In particular, **10h** displayed a 2-fold increase in selectivity for ERAP1 compared to ERAP2, with respect to that of the initial hit, **4a**. Interestingly, compound **10j′** (R_1═hTyr and R_2═Trp), the topoisomer of ERAP1-inactive **4r**, exhibits an IC_{50} = 0.8 μM for ERAP1 with a ∼12-fold selectivity with respect to ERAP2. Similar to the 1,3-analogues, the use of Nle at R_1 (**10m**−**10o′**) in combination with Tyr or Trp at R_2 provided the most potent ERAP2 and IRAP inhibitors. Among them, **10n**, with IC_{50} = 755 nM for ERAP2, is the most selective inhibitor against ERAP1 (>130-fold), and **10o′** is the most potent inhibitor of ERAP2 (IC_{50} = 237 nM). The corresponding benzyl ester of the latter, **10o**, displayed a higher potency for IRAP (IC_{50} = 438 nM) with respect to ERAP2 (IC_{50} = 709 nM). Finally, **10q** with R_1═Arg, the para-isomer of potent ERAP2/IRAP inhibitor **4x**, provided an equipotent inhibitor of the three enzymes (IC_{50} = 1.4−2.6 μM).

Overall, the in vitro evaluation of the designed DABA derivatives revealed several potent inhibitors for the three M1 aminopeptidases. ERAP1 appears to be the most challenging target in terms of inhibitor potency and selectivity, with **4u**

DOI: 10.1021/jm501867s
J. Med. Chem. 2015, 58, 1524−1543

(IC_{50} = 0.92 μM) and **10j′** (IC_{50} = 0.80 μM) being the most effective inhibitors and **10h** being the most selective with respect to ERAP2 (~20-fold). On the other hand, our optimization efforts resulted in significantly more potent inhibitors of ERAP2 (**10o′**, IC_{50} = 237 nM) and IRAP (**4u**, IC_{50} = 105 nM). In addition, we identified two remarkably selective inhibitors, **10n**, displaying IC_{50} = 755 nM for ERAP2 and IC_{50} > 100 μM for ERAP1, and **4s**, with IC_{50} = 1.3 μM for IRAP and IC_{50} > 100 μM for both ERAP1 and ERAP2. Conclusively, the inhibitory potency of the synthesized compounds revealed that Nle as the R_1 and Trp as the R_2 substituents provided the most potent inhibitors for the three aminopeptidases. It is possible that the linear side chain of Nle is easily accommodated within the S1 pocket and facilitates the proper orientation of the inhibitors in both topologies of the DABA derivatives. The indole ring of Trp is most probably mediating key aromatic interactions at the S-primed subsites in addition to potential hydrogen-bonding interactions. Similar observations were drawn from the crystallographic structure of ERAP1 in complex with a phosphinic transition state analogue tripeptide comprising a Trp residue, which was found to be stacked with catalytic Y438.[21]

Structure–Activity Relationships. Recent crystallographic studies revealed that ERAP1 can adopt at least two distinct conformational states that involve large interdomain motions, a closed, active-form (Figure 1a) and an open, inactive conformation that exposes a large internal peptide-binding cavity to the solvent.[25] Although ERAP2 has been crystallized in the closed conformation only, the absence of substrate access into the active site in the published structure suggests that ERAP2 should be able to adopt open conformations as well.[26] These two states differ in the organization of key active site residues and the adjacent S1 specificity pocket, which is disordered in the open state, making inhibitor design a challenging task.[14] Specifically, the conserved ERAP1 residue F433 that comprises the bottom of the S1 pocket as well as the catalytic Y438 are both disordered or dislocated in the open-state crystal structure.[27]

It is therefore plausible that inhibitors that target these aminopeptidases may form initial interactions inside the active site at different configurations than those expected by analyzing the closed crystallographic structures. This may be exemplified by a lack of a strong zinc binding group serving as anchor point. As a result, molecular docking calculations of the synthesized compounds reveal multiple putative binding poses inside the active sites of all three aminopeptidases. Still, the most potent inhibitors display a common binding motif among the top-ranked predicted conformations, where the carbonyl group of R_1 is bound to zinc so that the R_1 side chain can be accommodated within the S1 pocket (Figure 1c). In such conformation, the α-amino acid terminal amine displays salt bridge interactions with two conserved glutamates, E183/200/295 and E320/337/431 (residue numbering of ERAP1/ERAP2/IRAP, respectively), and the free aniline could provide an additional hydrogen bond with the catalytic E354/371/465 residue. It is therefore possible that only the best inhibitors bind in the expected conformation through an induced-fit mechanism that promotes correct folding of the APA active site.

The docked conformation of the most potent ERAP1 inhibitor, **10j′**, displays the side chain of its hTyr stacked above F433 inside the S1 pocket and, at the same time, forms a hydrogen bond with the backbone NH of S869 (Figure 2a), a

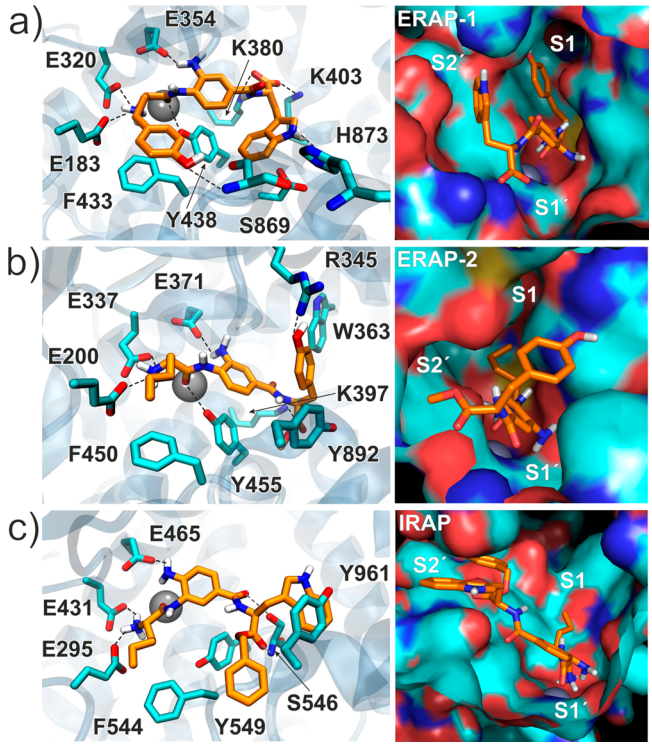

Figure 2. Close-up view of the active site from molecular models of (a) ERAP1–**10j′**, (b) ERAP2–**10n**, and (c) IRAP–**4u** complexes. The inhibitors are shown with carbon atoms in orange, and the key interacting residues, with cyan carbons. Potential hydrogen bonds are indicated with dashed lines, and the surface representations illustrate the three potential subsites of the enzymes.

residue that belongs to the C-terminal domain IV. The indole ring of **10j′** could interact with the H873 residue of domain IV, whereas its terminal carboxylic acid might form salt bridges with K308 and K403. Considering the bound conformation of the most selective inhibitor of ERAP2 (>100-fold with respect to ERAP1), **10n** is predicted to bind in a similar orientation as that for **10j′**. However, the phenolic ring in **10n** could be accommodated between the aromatic side chains of Y892 and W363 so that a hydrogen bond is formed between its hydroxylate group and R345 of ERAP2 (Figure 2b). The nonconserved W363 residue of ERAP2 corresponds to G346 of ERAP1 and therefore such an interaction might not be possible between ERAP1 and **10n**. The most potent IRAP inhibitor, **4u**, is predicted to interact mostly with conserved residues and thus displays low-micromolar affinity for ERAP1 and ERAP2 as well. The high binding affinity of **4u** for IRAP (105 nM) can be attributed to a potential stacking interaction of the indole moiety with Y961 and the two hydrogen bonds with S546 (Figure 2c). The terminal benzyl group of **4u** is predicted to provide minor contacts; therefore, the corresponding deprotected analogue, **4u′**, displayed a marginally lower binding affinity for IRAP (296 nM).

Biological Evaluation of Inhibitors. To assess the biological efficacy of this group of inhibitors we utilized two specialized cellular assays that relate to the function of the human innate and adaptive immune responses. It has been recently demonstrated that macrophages respond to the inflammatory modulator interferon-γ in combination with lipopolysaccharide (LPS), which is a component of the outer membrane of Gram-negative bacteria, by secreting ERAP1 in a

DOI: 10.1021/jm501867s
J. Med. Chem. 2015, 58, 1524–1543

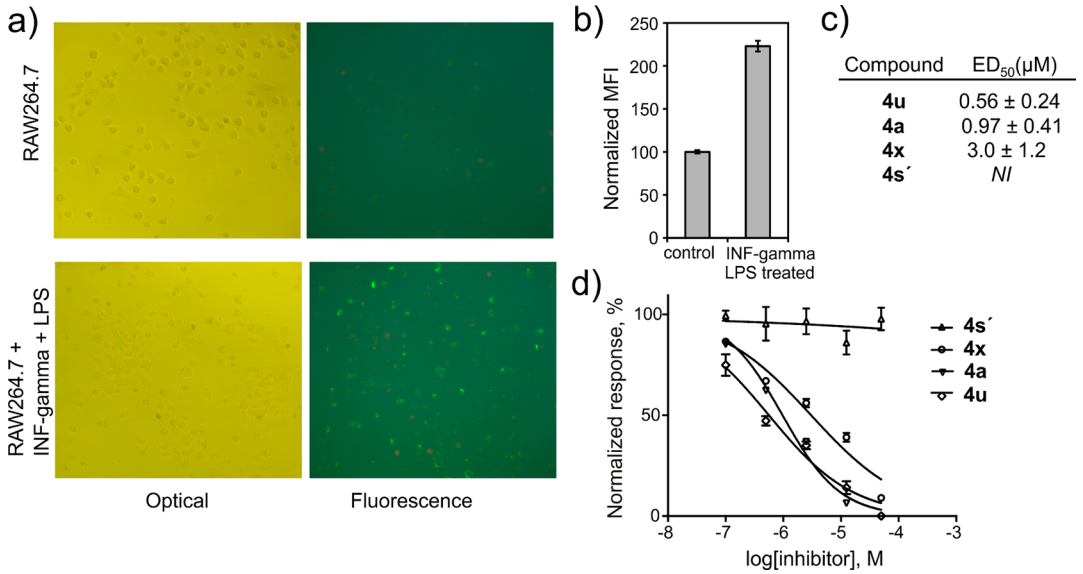

Figure 3. (a) Effect of interferon-γ and LPS on the phagocytic activity of RAW264.7 macrophages as followed by the internalization of fluorescent latex beads. (b) Fluorescence enhancement due to macrophage activation. (c, d) Reduction of fluorescence enhancement due to inhibition of phagocytosis by the ERAP1 inhibitors and the calculated ED_{50} values.

TLR-dependent manner.[10,11] The aminopeptidase activity of the secreted ERAP1 induces the enhancement of phagocytosis by macrophages, which can be followed by the internalization of fluorescently labeled latex beads (Figure 3a). To evaluate the effect of the inhibitors on this process, we measured the total cell fluorescence in stimulated and unstimulated cells. Total fluorescence enhancement upon macrophage stimulation was in the range of 100−150%, which is a sufficient signal change to detect inhibitory effects (Figure 3b). Adding compounds 24 h premeasurement revealed a dose dependent reduction in phagocytosis with calculated ED_{50} values (Figure 3c,d) that correspond well to the in vitro IC_{50} values calculated for ERAP1 using recombinant protein, suggesting that the biological effect was indeed mediated through the inhibition of ERAP1.

Furthermore, we evaluated the effectiveness of the most potent IRAP inhibitor, **4u**, on blocking cross-presentation by bone marrow-derived DCs (BMDCs). To assess the specificity of the inhibitor, we utilized BMDCs from both wild-type and IRAP knockout mice. We first confirmed that **4u** is able to inhibit mouse IRAP using mouse recombinant enzyme and discovered that this compound is 2-fold more effective for mouse IRAP ($IC_{50,mouse}$ = 52 nM, Supporting Information Figure S1) compared to that for human IRAP ($IC_{50,human}$ = 105 nM). Mouse BMDCs were first exposed to yeast cells expressing surface ovalbumin and then added to $CD8^+$ T cells from the lymph nodes of transgenic mice expressing a T cell receptor specific for the peptide ovalbumin247−254. T cell activation by the cross-presented epitope was read out as IL-2 secretion (Figure 4a). The same experiment was performed in the presence of increasing doses of **4u** (Figure 4b). In the presence of the inhibitor, cross-presentation was reduced in a dose-dependent manner with an ED_{50} of 6.5 nM. No effect was seen when we used BMDCs from IRAP knockout mice, indicating that the effect is specific for the IRAP-dependent cross-presentation pathway. The surprisingly high effectiveness of the inhibitor in this setting may be related to the compartmentalization of the cross-presentation process in which high local concentrations may be obtained due to continued inhibitor internalization into phagosomes and endosomes.

To date, only a series of phosphinic pseudopeptide transition state analogues has been reported as potent inhibitors of all three APAs,[21] albeit with low selectivity among the three enzymes. Specifically, the most potent inhibitor displayed IC_{50} values of 33, 11, and 30 nM for ERAP1, ERAP2, and IRAP, respectively. On the basis of the observation that peptide inhibitors of IRAP can enhance cognitive functions, peptidomimetic analogues of angiotensin IV have been designed using a wide range of synthetic approaches.[28−30] Among the most potent angiotensin IV mimetics reported, a series of macrocyclic compounds attained inhibition constants as low as 1.8 nM for IRAP.[30] With regard to small molecule inhibitors of IRAP, a series of benzopyran compounds that had been identified through a virtual screening approach using a homology model of IRAP[31] led to the development of the first lead compound with K_i = 30 nM through a medicinal chemistry campaign.[32] Recently, a series of arylsulfonamides was identified as being moderate inhibitors of IRAP, with the most potent exhibiting IC_{50} = 1.1 μM.[33] These IRAP inhibitors, however, have either not been tested for their ability to inhibit ERAP1 and ERAP2 or have been tested and found not to be active.[31] As a result, the 3,4-diaminobenzoic acid derivatives described here appear to constitute not only an alternative potent chemical tool for controlling APA activity but also one with very good selectivity properties.

■ CONCLUSIONS

In summary, we have investigated the ability of 3,4-diaminobenzoic acid derivatives to act as inhibitors of three critical aminopeptidases involved in the human innate and adaptive immune response, ERAP1, ERAP2, and IRAP. Our analysis revealed potent inhibitors for ERAP2 and IRAP as well as excellent selectivity profiles for all three enzymes. Furthermore, our analysis confirmed previously hypothesized difficulties in the rational design of inhibitors for this class of enzymes based on existing crystal structures, especially for ERAP1, possibly due to the conformational heterogeneity of

DOI: 10.1021/jm501867s
J. Med. Chem. 2015, 58, 1524−1543

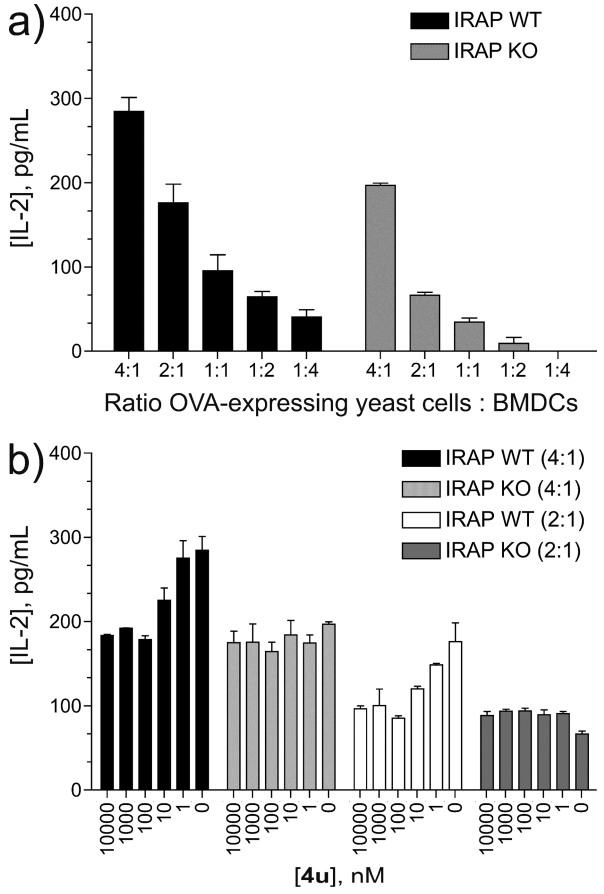

Figure 4. (a) Murine BMDCs from either wild-type or IRAP knockout mice were exposed to several ratios of ovalbumin-expressing yeast cells and subsequently to $CD8^+$ T cells purified from lymph nodes of OT-I mice. T cell activation was evaluated by measuring the IL-2 concentration in the culture supernatant. (b) The same experiment was repeated in the presence of increasing concentrations of **4u**. Note that titration of the inhibitor affected only wild-type, not IRAP knockout, cells and reduced the response of the wild-type cells to the levels of the IRAP knockout cells, indicating complete inhibition of the IRAP-dependent cross-presentation pathway.

this enzyme that greatly affects the folding of the S1 specificity pocket. Our best compounds were found to be active in specialized cellular assays related to their biological functions of the targeted enzymes in regulation of the adaptive and innate immune responses. We conclude that this class of compounds may find important applications in the regulation of inflammatory human immune responses for the treatment of a variety of major human diseases, varying from viral infections to cancer and autoimmunity. More specifically, ERAP1 inhibitors such as **4a** may be useful for reducing inflammation by controlling macrophage activation[11] and selective ERAP2 inhibitors like **10n** may be useful for controlling autoimmune responses brought about by high ERAP2 expression, such as that seen in birdshot chorioretinopathy,[34] or for enhancing immune responses toward immune-evading cancer cells.[35] Finally, potent IRAP inhibitors such as **4u** or **4u′** may find uses in controlling inflammatory autoimmune diseases or as cognitive enhancers.[36,32]

EXPERIMENTAL SECTION

Materials and General Procedures. Unless otherwise noted, all solvents and reagents for organic synthesis were obtained from commercial suppliers and used without further purification. Reactions requiring anhydrous conditions were carried out in flame-dried (vacuum <0.5 Torr) glassware, using anhydrous, freshly distilled solvents and under an Ar atmosphere. All reactions were stirred with Teflon-coated magnetic stir bars, and temperatures were measured externally. Yields refer to chromatographically and spectroscopically (^{1}H NMR) homogeneous materials. Reactions were monitored by thin-layer chromatography (TLC) carried out on 0.25 mm silica gel plates (60 F254, E. Merck). Silica gel (60, particle size: 0.040−0.063 mm, E. Merck) was used for flash column chromatography. NMR spectra were recorded on a Bruker Avance DRX-500 instrument at 298 K using residual undeuterated solvent for ^{1}H NMR [δ_H = 7.26 ($CHCl_3$), 2.50 (DMSO-d_5), and 3.31 (MeOH-d_3) ppm] and ^{13}C deuterated solvent for ^{13}C NMR [δ_C = 77.16 ($CDCl_3$), 39.52 (DMSO-d_5), and 49.00 (MeOH-d_4) ppm] as an internal reference. The following abbreviations were used to designate the multiplicities: s, singlet; d, doublet; t, triplet; q, quartet; m, multiplet; and br, broad. Quantitation of the final compounds was achieved using an internal standard of 2,5-dimethylfuran (DMFu, 0.1 mM in MeOD).[37] High-resolution mass spectra (HRMS) were measured on Agilent 6224 Accurate Mass TOF LC/MS at the Faculty of Chemistry and Chemical Technology, University of Ljubljana. Compounds were purified by reversed-phase HPLC on a C18 chromolith column (Merck) using a 0−50% (v/v) acetonitrile gradient in water containing 0.05% TFA while following the absorbance at 257 nm. The purity of all final compounds employed in the biological assays was greater than 95%, and the structures of the synthesized compounds were determined by ^{1}H NMR, ^{13}C NMR, and high-resolution mass spectroscopy (HRMS).

General Methods for the Synthesis of the Inhibitors. Amino Acid Coupling (Method A). A mixture of **1** (1.0 equiv), the desired *N*-Boc protected amino acid (1.1 equiv), HBTU (2.0 equiv), and DIEA (3.0 equiv) in anhydrous DMF (0.25 mM) was stirred under an Ar atmosphere at ambient temperature for 4 h. Similarly, a mixture of the carboxylic acid derivative of **2** or **7** (1.0 equiv), the desired *O*-Me or *O*-Bn protected amino acid (1.5 equiv), HBTU (3.0 equiv), and DIEA (4.0 equiv) in anhydrous DMF (0.25 mM) was stirred under an Ar atmosphere at ambient temperature for 8−12 h. For the preparation of the 1,4-substituted compounds, a mixture of **5** or **8** (1.0 equiv), the *N*-Boc protected amino acid (2.0 equiv), HATU (3.0 equiv), and DBU (4.0 equiv) in anhydrous DMF (0.25 mM) was stirred under an Ar atmosphere at ambient temperature for 24−36 h. The reaction mixture was then diluted with EtOAc and washed sequentially with aqueous HCl 1.0 N, sat. $NaHCO_3$, and sat. NaCl. Consequently, the solvent was evaporated under reduced pressure to provide the crude product, which was purified using a gradient of EtOAc in hexanes to yield the desired products in yields of 45−92%.

Saponification of Methyl Esters (Method B). The desired compound was dissolved in a mixture of 1:1 dioxane/aqueous LiOH 1.0 M (20 equiv) under rigorous stirring. After 3−6 h (monitored by TLC) at ambient temperature, the mixture was diluted with aqueous sat. NaCl and the organic solvent was evaporated. The remaining aqueous solution (pH 12) was washed with EtOAc and then acidified with HCl 1.0 N until no further precipitation could be observed (pH 2). The aqueous phase was then extracted three times with EtOAc, and the combined organic extracts were dried with $MgSO_4$, filtered, and washed with EtOAc. After evaporating the solvents and drying under high vacuum, the product was obtained at yields of 87−95% and purity > 95% (NMR).

General Procedure for the Deprotection of *O*-Bn and *N*-Cbz Groups (Method C). The desired compound (0.1 mmol) was dissolved in MeOH (4 mL, 0.025 mM), and the solution was degassed under an Ar atmosphere. A catalytic amount of activated Pd/C 10% was added and degassed under Ar, followed by the introduction of H_2 gas. The mixture was stirred under H_2 at ambient temperature for 1−2 h (monitored by TLC) and then filtered through Celite and washed with MeOH. The resulting product was acquired in yields of 90−95%.

General Procedure for the Deprotection of *N*-Boc and *O*-tBu Groups (Method D). The desired compound (0.1 mmol) was dissolved in a mixture of CH_2Cl_2/TFA (2:1 mL, 0.033 mM) and

DOI: 10.1021/jm501867s
J. Med. Chem. 2015, 58, 1524−1543

stirred at ambient temperature for 20−40 min (monitored by TLC). Consequently, the solvents were evaporated, and the product was treated with HCl 1.0 N (0.5 mL). The solvents were evaporated using toluene (2 × 2 mL) to azeotrop the remaining aqueous solution and dried under high vacuum overnight to yield the hydrochloric salt of the amine in yields of 95−99%.

Methyl 4-Amino-3-((*tert*-butoxycarbonyl)amino)benzoate (5). To a stirred solution of **1** (500 mg, 3.0 mmol) and Gu·HCl (45 mg, 0.45 mmol) in 5 mL of EtOH was added $(Boc)_2O$ (650 mg, 3.0 mmol), and the mixture was heated at 45 °C for 40 min. Subsequently, ethanol was evaporated under reduced pressure, and the reaction mixture was redissolved in EtOAc and washed sequentially with aqueous HCl 1.0 N, sat. $NaHCO_3$, and sat. NaCl. The organic layer was evaporated under reduced pressure to provide the crude product, which was purified using a gradient of 35−65% EtOAc in hexanes to yield the *N*-Boc protected amine **5** (665 mg, 2.5 mmol, 83%). ^{1}H NMR (500.13 MHz, $CDCl_3$): δ 7.83 (s, 1H), 7.56 (dd, J = 8.4, 1.7 Hz, 1H), 6.76 (s, 1H), 6.58 (d, J = 8.4 Hz, 1H), 4.39 (s, 2H), 3.74, (s, 3H), 1.41 (s, 9H). ^{13}C NMR (125.76 MHz, $CDCl_3$): δ 167.0, 154.2, 145.8, 128.3, 127.6, 122.7, 119.4, 115.5, 80.5, 51.5, 28.1, 28.1, 28.1.

Saponification of methyl ester of **5** using method B yielded **7**, as reported in the literature.[38]

(*S*)-Methyl 4-Amino-3-(2-amino-3-(4-(benzyloxy)phenyl)-propanamido)benzoate (3a).

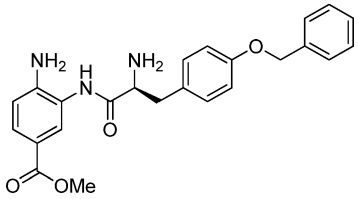

^{1}H NMR (500.13 MHz, MeOH-d_4): δ 7.82 (d, J = 8.4 Hz, 1H), 7.65 (s, 1H), 7.47−7.42 (m, 2H), 7.38−7.32 (m, 2H), 7.31−7.25 (m, 3H), 7.10−7.06 (m, 1H), 7.04 (d, J = 8.5 Hz, 2H), 5.16−5.08 (m, 2H), 4.32−4.25 (m, 1H), 3.85 (s, 3H), 3.25−3.17 (m, 2H). ^{13}C NMR (125.76 MHz, MeOH-d_4): δ 171.9, 169.4, 160.1, 147.1, 138.6, 131.8, 131.8, 131.8, 130.5, 130.5,129.6, 129.5, 129.5, 128.9, 128.6, 127.5, 127.5, 119.3, 116.7, 116.7, 71.1, 56.4, 52.6, 38.0. HRMS (ESI): m/z calcd for $C_{24}H_{25}N_3O_4$ + H^+ [M + H^+], 420.1918; found, 420.1922.

(*S*)-4-Amino-3-(2-amino-3-(4-(benzyloxy)phenyl)-propanamido)benzoic Acid (3a′).

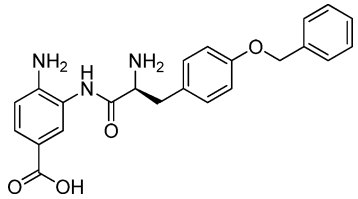

^{1}H NMR (500.13 MHz, MeOH-d_4): δ 7.90 (d, J = 8.3 Hz, 1H), 7.71 (s, 1H), 7.46−7.41 (m, 2H), 7.38−7.32 (m, 2H), 7.31−7.25 (m, 3H), 7.23 (dd, J = 8.3, 2.5 Hz, 1H), 7.03 (d, J = 8.2 Hz, 2H), 5.18−5.03 (m, 2H), 4.34−4.28 (m, 1H), 3.28−3.23 (m, 1H), 3.22−3.16 (m, 1H). ^{13}C NMR (125.76 MHz, MeOH-d_4): δ 169.5, 168.5, 160.0, 139.6, 138.6, 131.8, 131.8, 131.8, 130.6, 129.6, 129.5, 129.5, 128.9, 128.6, 128.6, 127.5, 127.0, 121.2, 116.7, 116.7, 71.0, 56.3, 37.8. HRMS (ESI): m/z calcd for $C_{23}H_{23}N_3O_4$ + H^+ [M + H^+], 406.1761; found, 406.1767.

(*S*)-Methyl 4-Amino-3-(2-amino-3-(4-hydroxyphenyl)-propanamido)benzoate (3b).

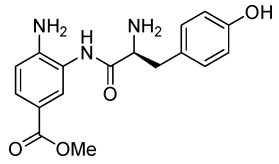

^{1}H NMR (500.13 MHz, MeOH-d_4): δ 7.90 (br.d, 1H), 7.71 (s, 1H), 7.28−7.23 (m, 1H), 7.18 (d, J = 8.3 Hz, 2H), 6.83 (d, J = 8.3 Hz, 2H), 4.33−4.27 (m, 1H), 3.91 (s, 3H), 3.26−3.11 (m, 2H). ^{13}C NMR (125.76 MHz, MeOH-d_4): δ 174.0, 169.7, 167.3, 158.5, 131.7, 131.7, 130.2, 129.3, 128.5, 126.9, 125.9, 121.6, 117.0, 117.0, 56.5, 52.8, 37.8. HRMS (ESI): m/z calcd for $C_{17}H_{19}N_3O_4$ + H^+ [M + H^+], 330.1448; found, 330.1444.

(*S*)-4-Amino-3-(2-amino-3-(4-hydroxyphenyl)propanamido)-benzoic Acid (3b′).

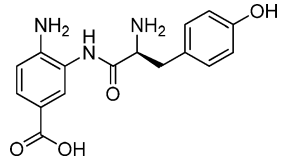

^{1}H NMR (500.13 MHz, MeOH-d_4): δ 7.90 (br.d, 1H), 7.81 (s, 1H), 7.25−7.21 (m, 1H), 7.19 (d, J = 8.4 Hz, 2H), 6.83 (d, J = 8.4 Hz, 2H), 4.33−4.25 (m, 1H), 3.30−3.24 (m, 1H), 3.16−3.08 (m, 1H). ^{13}C NMR (125.76 MHz, MeOH-d_4): δ 179.0, 169.6, 158.5, 140.5, 131.7, 131.7, 130.6, 129.5, 126.9, 125.8, 121.4, 121.4, 117.0, 117.0, 56.5, 37.9. HRMS (ESI): m/z calcd for $C_{16}H_{17}N_3O_4$ + H^+ [M + H^+], 316.1292; found, 316.1298.

(*S*)-Methyl 4-Amino-3-(2-amino-4-(4-(benzyloxy)phenyl)-butanamido)benzoate (3c).

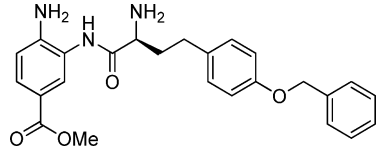

^{1}H NMR (500.13 MHz, MeOH-d_4): δ 7.95 (s, 1H), 7.90 (dd, J = 8.4, 1.8 Hz, 1H), 7.42−7.37 (m, 2H), 7.37−7.32 (m, 2H), 7.32−7.25 (m, 2H), 7.20 (d, J = 8.6 Hz, 2H), 6.92 (d, J = 8.6 Hz, 2H), 5.02 (s, 2H), 4.33−4.26 (m, 1H), 3.87 (s, 3H), 2.84−2.74 (m, 2H), 2.42−2.33 (m, 1H), 2.32−2.24 (m, 1H). ^{13}C NMR (125.76 MHz, MeOH-d_4): δ 169.9, 167.3, 158.9, 138.8, 133.5, 130.4, 130.4, 130.1, 130.1, 129.4, 129.4, 128.9, 128.8, 128.5, 128.5, 127.9, 127.3, 122.1, 116.2, 116.2, 71.1, 55.0, 52.8, 34.5, 31.3. HRMS (ESI): m/z calcd for $C_{25}H_{27}N_3O_4$ + H^+ [M + H^+], 434.2074; found, 434.2079.

(*S*)-Methyl 4-Amino-3-(2-amino-4-(4-hydroxyphenyl)-butanamido)benzoate (3d).

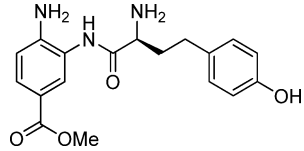

^{1}H NMR (500.13 MHz, MeOH-d_4): δ 7.93 (s, 1H), 7.86 (d, J = 8.4 Hz, 1H), 7.21 (d, J = 8.4 Hz, 1H), 7.10 (d, J = 8.3 Hz, 2H), 6.73 (d, J = 8.3 Hz, 2H), 4.30−4.22 (m, 1H), 3.88 (s, 3H), 2.80−2.68 (m, 2H), 2.41−2.28 (m, 1H), 2.28−2.20 (m, 1H). ^{13}C NMR (125.76 MHz, MeOH-d_4): δ 169.9, 167.6, 157.1, 140.4, 131.9, 130.3, 130.3, 130.2, 129.1, 126.7, 125.8, 121.0, 116.5, 116.5, 54.9, 52.7, 34.8, 31.3. HRMS (ESI): m/z calcd for $C_{18}H_{21}N_3O_4$ + H^+ [M + H^+], 344.1605; found, 344.1607.

(*S*)-Methyl 4-Amino-3-(2-amino-4-methylpentanamido)-benzoate (3e).

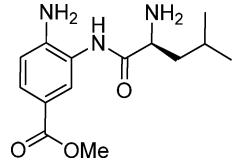

^{1}H NMR (500.13 MHz, MeOH-d_4): δ 7.94 (s, 1H), 7.88 (d, J = 8.0, 1H), 7.21 (d, J = 8.0 Hz, 1H), 4.25−4.15 (m, 1H), 3.88 (s, 3H), 1.97−1.76 (m, 3H), 1.11−1.05 (m, 6H). ^{13}C NMR (125.76 MHz, MeOH-d_4): δ 170.6, 167.6, 140.6, 130.4, 129.2, 126.7, 125.7, 121.0, 53.5, 52.7, 41.5, 25.6, 23.3, 21.9. HRMS (ESI): m/z calcd for $C_{14}H_{21}N_3O_3$ + H^+ [M + H^+], 280.1656; found, 280.1659.

DOI: 10.1021/jm501867s
J. Med. Chem. 2015, 58, 1524−1543

(*S*)-4-Amino-3-(2-amino-4-methylpentanamido)benzoic Acid (3e′).

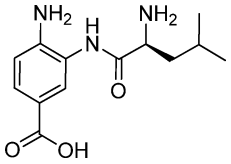

^{1}H NMR (500.13 MHz, MeOH-d_4): δ 8.08−7.88 (m, 2H), 7.42−7.35 (m, 1H), 4.27−4.19 (m, 1H), 2.01−1.75 (m, 3H), 1.11−1.05 (m, 6H). ^{13}C NMR (125.76 MHz, MeOH-d_4): δ 170.7, 168.2, 136.5, 130.4, 129.4, 129.1, 123.0, 115.4, 53.5, 41.4, 25.6, 23.3, 21.9. HRMS (ESI): m/z calcd for $C_{13}H_{19}N_3O_3$ + H^+ [M + H^+], 266.1499; found, 266.1500.

(*S*)-Methyl 4-Amino-3-(2-aminohexanamido)benzoate (3f).

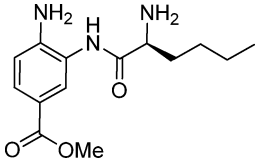

^{1}H NMR (500.13 MHz, MeOH-d_4): δ 7.99 (d, J = 1.9 Hz, 1H), 7.90 (dd, J = 8.4, 1.9 Hz, 1H), 7.35 (d, J = 8.4 Hz, 1H), 4.34−4.16 (m, 1H), 3.89 (s, 3H), 2.15−1.94 (m, 2H), 1.61−1.36 (m, 4H), 1.09−0.87 (m, 3H). ^{13}C NMR (125.76 MHz, MeOH-d_4): δ 170.4, 167.1, 136.2, 130.0, 129.1, 128.8, 123.3, 115.3, 55.1, 52.9, 32.2, 28.1, 23.4, 14.0. HRMS (ESI): m/z calcd for $C_{14}H_{21}N_3O_3$ + H^+ [M + H^+], 280.1656; found, 280.1655.

(*S*)-Methyl 4-Amino-3-(2-amino-5-guanidinopentanamido)-benzoate (3g).

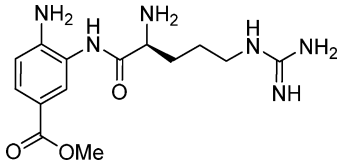

^{1}H NMR (500.13 MHz, MeOH-d_4): δ 8.11 (s, 1H), 7.97 (d, J = 8.3 Hz, 1H), 7.53−7.46 (m, 1H), 4.40−4.28 (m, 1H), 3.92 (s, 3H), 3.37−3.32 (m, 2H), 2.27−2.20 (m, 1H), 2.16−2.07 (m, 1H), 1.91−1.80 (m, 2H). ^{13}C NMR (125.76 MHz, MeOH-d_4): δ 170.0, 166.9, 158.6, 144.8, 130.2, 129.9, 128.7, 124.3, 124.2, 54.6, 53.0, 41.8, 29.6, 25.7. HRMS (ESI): m/z calcd for $C_{14}H_{22}N_6O_3$ + H^+ [M + H^+], 323.1826; found, 323.1818.

(*S*)-4-Amino-3-(2-amino-5-guanidinopentanamido)benzoic Acid (3g′).

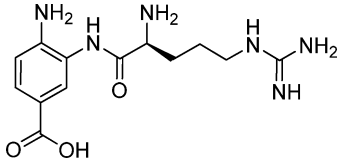

^{1}H NMR (500.13 MHz, MeOH-d_4): δ 8.12 (br.s, 1H), 8.04−7.97 (m, 1H), 7.60−7.47 (m, 1H), 4.40−4.28 (m, 1H), 3.38−3.32 (m, 2H), 2.29−2.20 (m, 1H), 2.15−2.06 (m, 1H), 1.90−1.80 (m, 2H). ^{13}C NMR (125.76 MHz, MeOH-d_4): δ 170.0, 167.8, 158.6, 131.7, 130.6, 130.1, 128.8, 124.7, 124.4, 54.6, 41.8, 29.6, 25.7. HRMS (ESI): m/z calcd for $C_{13}H_{20}N_6O_3$ + H^+ [M + H^+], 309.1670; found, 309.1677.

(*S*)-Methyl 5-Amino-2-(4-amino-3-((*S*)-2-amino-4-phenylbutanamido)benzamido) pentanoate (4d).

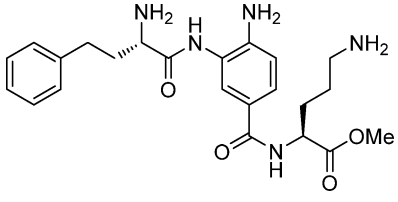

^{1}H NMR (500.13 MHz, MeOH-d_4): δ 7.73 (s, 1H), 7.60 (dd, J = 8.4, 1.9 Hz, 1H), 7.30−7.14 (m, 5H), 6.84 (d, J = 8.4 Hz, 1H), 4.64−4.56 (m, 1H), 3.91−3.83 (m, 1H), 3.72 (s, 3H), 3.02−2.89 (m, 2H), 2.86−2.72 (m, 2H), 2.28−2.19 (m, 1H), 2.14−1.97 (m, 2H), 1.94−1.68 (m, 3H). ^{13}C NMR (125.76 MHz, MeOH-d_4): δ 173.9, 173.5, 169.9, 148.1, 142.1, 129.6, 129.5, 129.4, 128.3, 127.7, 127.3, 123.2, 122.9, 122.4, 116.6, 55.6, 53.6, 52.8, 40.3, 36.6, 32.7, 29.3, 25.3. HRMS (ESI): m/z calcd for $C_{23}H_{31}N_5O_4$ + H^+ [M + H^+], 442.2449; found, 442.2450.

(*S*)-5-Amino-2-(4-amino-3-((*S*)-2-amino-4-phenylbutanamido)benzamido)pentanoic Acid (4d′).

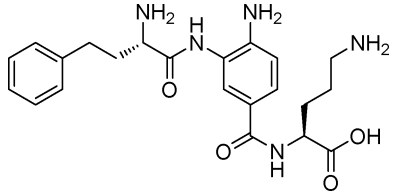

^{1}H NMR (500.13 MHz, MeOH-d_4): δ 7.68 (s, 1H), 7.56 (dd, J = 8.4, 1.9 Hz, 1H), 7.32−7.09 (m, 5H), 6.81 (d, J = 8.4 Hz, 1H), 4.49−4.40 (m, 1H), 3.90−3.75 (m, 1H), 2.88−2.72 (m, 2H), 2.32 (s, 1H), 2.26−2.20 (m, 1H), 2.17−2.13 (m, 1H), 2.12−2.03 (m, 1H), 2.00−1.84 (m, 4H). ^{13}C NMR (125.76 MHz, MeOH-d_4): δ 173.4, 173.3, 169.4, 147.8, 142.1, 129.6, 129.5, 129.4, 128.1, 127.5, 127.3, 123.7, 123.1, 122.5, 116.7, 55.6, 51.4, 42.8, 36.7, 32.7, 28.9, 22.5. HRMS (ESI): m/z calcd for $C_{22}H_{29}N_5O_4$ + H^+ [M + H^+], 428.2292; found, 428.2299.

(*S*)-6-Amino-2-(4-amino-3-((*S*)-2-amino-3-phenylpropanamido)benzamido)hexanoic Acid (4e).

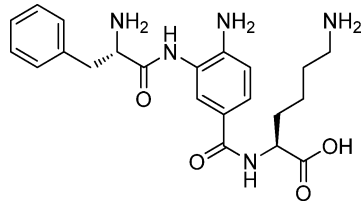

^{1}H NMR (500.13 MHz, MeOH-d_4): δ 7.92 (d, J = 8.3 Hz, 1H), 7.69 (s, 1H), 7.55 (d, J = 8.3 Hz, 1H), 7.47−7.34 (m, 5H), 4.64−4.55 (m, 1H), 4.53−4.46 (m, 1H), 3.51−3.43(m, 1H), 3.29−3.21 (m, 1H), 3.00−2.93 (m, 2H), 2.12−1.88 (m, 2H), 1.83−1.70 (m, 2H), 1.68−1.50 (m, 2H). ^{13}C NMR (125.76 MHz, MeOH-d_4): δ 175.0, 173.0, 169.8, 168.3, 135.4, 130.8, 130.7, 130.7, 130.3, 130.3, 129.1, 128.1, 127.1, 127.0, 125.0, 56.4, 54.2, 40.5, 38.4, 31.8, 28.1, 24.2. HRMS (ESI): m/z calcd for $C_{22}H_{29}N_5O_4$ + H^+ [M + H^+], 428.2292; found, 428.2289.

(*S*)-6-Amino-2-(4-amino-3-((*S*)-2-amino-3-(4-hydroxyphenyl)propanamido)benzamido)hexanoic Acid (4f).

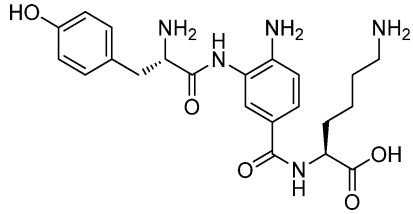

^{1}H NMR (500.13 MHz, MeOH-d_4): δ 7.92 (d, J = 8.3 Hz, 1H), 7.82 (s, 1H), 7.59 (d, J = 8.3 Hz, 1H), 7.25 (d, J = 8.1 Hz, 2H), 6.83 (d, J = 8.1 Hz, 2H), 4.62−4.55 (m, 1H), 4.49−4.38 (m, 1H), 3.45−3.37 (m, 1H), 3.19−3.10 (m, 1H), 3.02−2.91 (m, 2H), 2.09−1.90 (m, 2H), 1.85−1.70 (m, 2H), 1.67−1.48 (m, 2H). ^{13}C NMR (125.76 MHz, MeOH-d_4): δ 175.1, 170.0, 168.3, 158.3, 141.3, 131.8, 131.8, 129.6, 129.5, 128.1, 127.0, 125.9, 125.3, 117.0, 117.0, 56.6, 54.3, 40.5, 37.6, 31.7, 28.1, 24.2. HRMS (ESI): m/z calcd for $C_{22}H_{29}N_5O_4$ + H^+ [M + H^+], 444.2241; found, 444.2251.

DOI: 10.1021/jm501867s
J. Med. Chem. 2015, 58, 1524−1543

(*S*)-Methyl 6-Amino-2-(4-amino-3-((*S*)-2-amino-4-(4-hydroxyphenyl)butanamido) benzamido)hexanoate (4g).

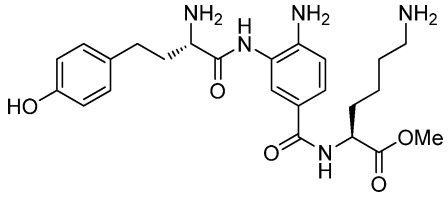

^{1}H NMR (500.13 MHz, MeOH-d_4): δ 7.99−7.85 (m, 2H), 7.54−7.46 (m, 1H), 7.13 (d, J = 8.2 Hz, 2H), 6.74 (d, J = 8.2 Hz, 2H), 4.64−4.54 (m, 1H), 4.38−4.32 (m, 1H), 3.74 (s, 3H), 3.00−2.90 (m, 2H), 2.83−2.69 (m, 2H), 2.44−2.33 (m, 1H), 2.32−2.22 (m, 1H), 2.06−1.87 (m, 2H), 1.80−1.68 (m, 2H), 1.64−1.46 (m, 2H). ^{13}C NMR (125.76 MHz, MeOH-d_4): δ 173.9, 170.2, 168.5, 157.0, 134.1, 133.1, 132.0, 130.4, 130.4, 130.1, 128.2, 127.0, 124.2, 116.4, 116.4, 55.1, 54.3, 52.9, 40.5, 34.8, 31.6, 31.4, 28.0, 24.1. HRMS (ESI): m/z calcd for $C_{24}H_{33}N_5O_5$ + H$^+$ [M + H$^+$], 472.2554; found, 472.2554.

(*S*)-Methyl 6-Amino-2-(4-amino-3-((*S*)-2-amino-4-(4-(benzyloxy)phenyl)butanamido) benzamido)hexanoate (4h).

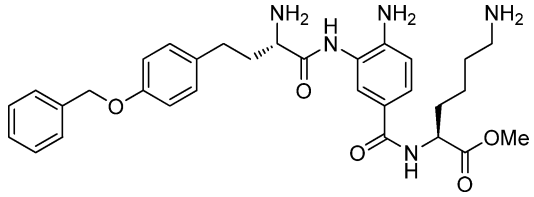

^{1}H NMR (500.13 MHz, MeOH-d_4): δ 8.05−7.93 (m, 2H), 7.67−7.57 (m, 1H), 7.50−7.19 (m, 7H), 7.00−6.88 (m, 2H), 5.04 (s, 2H), 4.66−4.56 (m, 1H), 4.46−4.31 (m, 1H), 3.82−3.68 (m, 3H), 3.02−2.90 (m, 2H), 2.88−2.77 (m, 2H), 2.52−2.24 (m, 2H), 2.10−1.88 (m, 2H), 1.82−1.68 (m, 2H), 1.67−1.46 (m, 2H). ^{13}C NMR (125.76 MHz, MeOH-d_4): δ 173.8, 170.3, 168.2, 158.9, 138.8, 135.9, 133.5, 131.6, 130.5, 130.5, 129.5, 129.5, 128.8, 128.8, 128.5, 128.5, 128.1, 126.9, 125.6, 116.2, 116.2, 71.0, 55.0, 54.4, 52.9, 40.5, 34.6, 31.6, 31.4, 28.0, 24.2. HRMS (ESI): m/z calcd for $C_{31}H_{39}N_5O_5$ + H$^+$ [M + H$^+$], 562.3024; found, 562.3026.

(*S*)-Methyl 6-Amino-2-(4-amino-3-((*S*)-2-amino-3-(benzyloxy)propanamido)benzamido)hexanoate (4i).

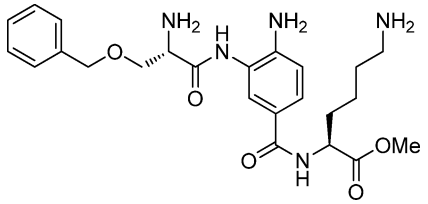

^{1}H NMR (500.13 MHz, MeOH-d_4): δ 7.95−7.83 (m, 2H), 7.48 (m, 1H), 7.45−7.23 (m, 5H), 4.74−4.64 (m, 2H), 4.64−4.56 (m, 1H), 4.55−4.50 (m, 1H), 4.11−4.02 (m, 2H), 3.79−3.68 (m, 3H), 2.99−2.90 (m, 2H), 2.07−1.86 (m, 2H), 1.82−1.68 (m, 2H), 1.64−1.48 (m, 2H). ^{13}C NMR (125.76 MHz, MeOH-d_4): δ 173.9, 168.5, 167.9, 138.4, 133.7, 129.6, 129.6, 129.2, 129.2, 129.2, 128.2, 127.2, 123.9, 123.8, 115.8, 74.6, 68.8, 55.2, 54.3, 52.9, 40.5, 31.7, 28.0, 24.2. HRMS (ESI): m/z calcd for $C_{24}H_{33}N_5O_5$ + H$^+$ [M + H$^+$], 472.2554; found, 472.2550.

(*S*)-Methyl 6-Amino-2-(4-amino-3-((*S*)-2-amino-4-methylpentanamido)benzamido) hexanoate (4j).

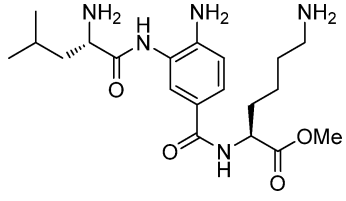

^{1}H NMR (500.13 MHz, MeOH-d_4): δ 7.94−7.80 (m, 2H), 7.42−7.35 (m, 1H), 4.63−4.57 (m, 1H), 4.28−4.22 (m, 1H), 3.78−3.70 (m, 3H), 2.98−2.90 (m, 2H), 2.09−1.79 (m, 5H), 1.78−1.69 (m, 2H), 1.64−1.45 (m, 2H), 1.11−1.06 (m, 6H). ^{13}C NMR (125.76 MHz, MeOH-d_4): δ 174.0, 170.8, 168.7, 151.2, 132.0, 128.6, 128.3, 127.3, 122.7, 54.2, 53.5, 52.8, 41.5, 40.5, 31.7, 28.0, 25.6, 24.2, 23.4, 21.9. HRMS (ESI): m/z calcd for $C_{20}H_{33}N_5O_4$ + H$^+$ [M + H$^+$], 408.2605; found, 408.2606.

(*S*)-6-Amino-2-(4-amino-3-((*S*)-2-amino-4-methylpentanamido)benzamido)hexanoic Acid (4j′).

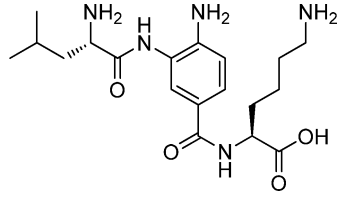

^{1}H NMR (500.13 MHz, MeOH-d_4): δ 7.96−7.85 (m, 2H), 7.46 (d, J = 8.2 Hz, 1H), 4.65−4.53 (m, 1H), 4.34−4.21 (m, 1H), 2.12−1.68 (m, 9H), 1.64−1.48 (m, 2H), 1.14−1.01 (m, 6H). ^{13}C NMR (125.76 MHz, MeOH-d_4): δ 175.1, 170.8, 168.5, 151.2, 129.5, 128.2, 127.2, 123.7, 123.5, 54.1, 53.6, 41.4, 40.6, 31.9, 28.1, 25.6, 24.2, 23.4, 21.9. HRMS (ESI): m/z calcd for $C_{19}H_{31}N_5O_4$ + H$^+$ [M + H$^+$], 394.2449; found, 394.2455.

(*S*)-Methyl 6-Amino-2-(4-amino-3-((*S*)-2-aminohexanamido)benzamido)hexanoate (4k).

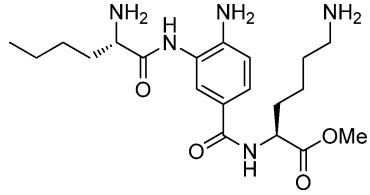

^{1}H NMR (500.13 MHz, MeOH-d_4): δ 7.92 (s, 1H), 7.88 (d, J = 8.4 Hz, 1H), 7.45 (d, J = 8.4 Hz, 1H), 4.63−4.57 (m, 1H), 4.28−4.22 (m, 1H), 3.76 (s, 3H), 2.99−2.92 (m, 2H), 2.15−2.06 (m, 1H), 2.05−1.96 (m, 2H), 1.95−1.88 (m, 1H), 1.78−1.68 (m, 2H), 1.62−1.43 (m, 6H), 1.03−0.97 (m, 3H). ^{13}C NMR (125.76 MHz, MeOH-d_4): δ 173.9, 170.5, 168.6, 134.3, 133.2, 129.5, 128.2, 127.1, 123.6, 55.1, 54.3, 52.9, 40.5, 32.3, 31.6, 28.2, 28.0, 24.2, 23.4, 14.1. HRMS (ESI): m/z calcd for $C_{20}H_{33}N_5O_4$ + H$^+$ [M + H$^+$], 408.2605; found, 408.2603.

(*S*)-Methyl 6-Amino-2-(4-amino-3-((*S*)-2-amino-5-guanidinopentanamido)benzamido)hexanoate (4l).

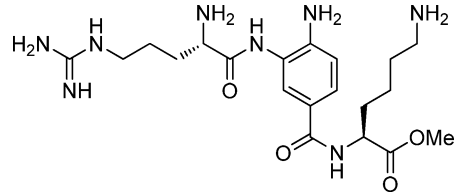

^{1}H NMR (500.13 MHz, MeOH-d_4): δ 8.00 (s, 1H), 7.88 (d, J = 8.2 Hz, 1H), 7.47−7.38 (m, 1H), 4.63−4.56 (m, 1H), 4.35−4.29 (m, 1H), 3.75 (s, 3H), 3.37−3.32 (m, 2H), 2.99−2.91 (m, 2H), 2.17−2.07 (m, 2H), 2.05−1.90 (m, 2H), 1.90−1.81 (m, 2H), 1.79−1.68 (m, 2H), 1.64−1.49 (m, 2H). ^{13}C NMR (125.76 MHz, MeOH-d_4): δ 174.0, 171.5, 169.9, 168.6, 158.6, 129.1, 128.3, 127.2, 123.4, 123.3, 54.7, 54.4, 52.9, 41.9, 40.7, 31.8, 29.8, 28.2, 25.8, 24.3. HRMS (ESI): m/z calcd for $C_{20}H_{34}N_8O_4$ + H$^+$ [M + H$^+$], 451.2776; found, 451.2777.

(*S*)-Benzyl 2-(4-Amino-3-((*S*)-2-amino-3-(4-hydroxyphenyl)-propanamido)benzamido)-3-methylbutanoate (4m).

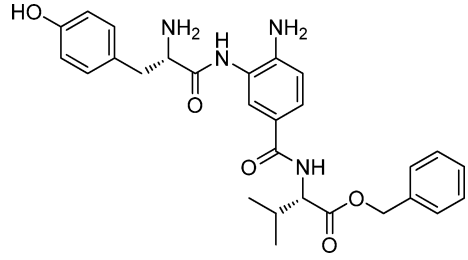

DOI: 10.1021/jm501867s
J. Med. Chem. 2015, 58, 1524−1543

^{1}H NMR (500.13 MHz, MeOH-d_4): δ 7.78 (d, J = 8.2 Hz, 1H), 7.69 (s, 1H), 7.41−7.29 (m, 6H), 7.21 (d, J = 8.3 Hz, 2H), 6.83 (d, J = 8.3 Hz, 2H), 5.26−5.21 (m, 1H), 5.19−5.14 (m, 1H), 4.51−4.46 (m, 1H), 4.39−4.33 (m, 1H), 3.36−3.32 (m, 1H), 3.16−3.08 (m, 1H), 2.32−2.22 (m, 1H), 1.06−0.94 (m, 6H). ^{13}C NMR (125.76 MHz, MeOH-d_4): δ 173.0, 169.9, 169.1, 167.3, 158.5, 137.2, 131.8, 131.8, 131.8, 129.6, 129.5, 129.5, 129.4, 129.4, 128.2, 127.3, 125.8, 122.9, 117.0, 117.0, 117.0, 67.9, 60.5, 56.5, 37.8, 31.7, 19.6, 19.2. HRMS (ESI): m/z calcd for $C_{28}H_{32}N_4O_5$ + H$^+$ [M + H$^+$], 505.2445; found, 505.2447.

(*S*)-2-(4-Amino-3-((*S*)-2-amino-3-(4-hydroxyphenyl)-propanamido)benzamido)-3-methylbutanoic Acid (4m′).

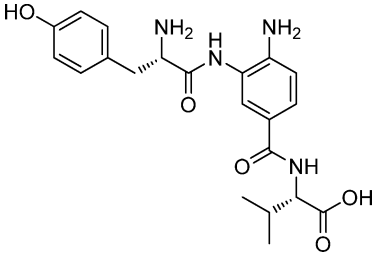

^{1}H NMR (500.13 MHz, MeOH-d_4): δ 7.86 (d, J = 8.3 Hz, 1H), 7.74 (s, 1H), 7.51 (d, J = 8.3 Hz, 1H), 7.22 (d, J = 8.3 Hz, 2H), 6.83 (d, J = 8.3 Hz, 2H), 4.52−4.46 (m, 1H), 4.43−4.37 (m, 1H), 3.40−3.33 (m, 1H), 3.18−3.07 (m, 1H), 2.35−2.24 (m, 1H), 1.09−1.01 (m, 6H). ^{13}C NMR (125.76 MHz, MeOH-d_4): δ 174.8, 169.9, 168.7, 167.1, 158.4, 135.4, 131.8, 131.8, 130.4, 128.1, 127.1, 125.8, 124.6, 117.0, 117.0, 60.1, 56.6, 37.7, 31.7, 19.7, 18.9. HRMS (ESI): m/z calcd for $C_{21}H_{26}N_4O_5$ + H$^+$ [M + H$^+$], 415.1976; found, 415.1982.

(*S*)-Methyl 2-(4-Amino-3-((*S*)-2-amino-3-(4-hydroxyphenyl)-propanamido) benzamido)-3-(4-hydroxyphenyl)propanoate (4n).

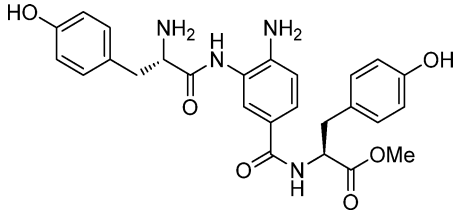

^{1}H NMR (500.13 MHz, MeOH-d_4): δ 7.70 (d, J = 8.3 Hz, 1H), 7.63 (s, 1H), 7.34 (dd, J = 8.4, 3.1 Hz, 1H), 7.21 (d, J = 8.4 Hz, 2H), 7.07 (d, J = 8.4 Hz, 2H), 6.83 (d, J = 8.4 Hz, 2H), 6.70 (d, J = 8.4 Hz, 2H), 4.80−4.74 (m, 1H), 4.38−4.32 (m, 1H), 3.72 (s, 3H), 3.23−3.15 (m, 2H), 3.14−3.07 (m, 1H), 3.06−2.99 (m, 1H). ^{13}C NMR (125.76 MHz, MeOH-d_4): δ 173.7, 169.9, 168.4, 158.5, 157.4, 132.9, 131.8, 131.8, 131.2, 131.2, 129.0, 128.9, 128.0, 127.2, 125.9, 123.1, 117.1, 117.1, 116.9, 116.3, 116.3, 56.6, 56.2, 52.8, 37.8, 37.4. HRMS (ESI): m/z calcd for $C_{26}H_{28}N_4O_6$ + H$^+$ [M + H$^+$], 493.2082; found, 493.2081.

(2*S*,3*R*)-Methyl 2-(4-Amino-3-((*S*)-2-amino-3-(4-hydroxyphenyl)propanamido)benzamido)-3-hydroxybutanoate (4o).

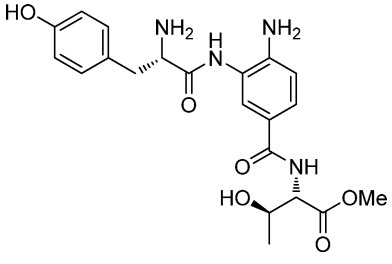

^{1}H NMR (500.13 MHz, MeOH-d_4): δ 7.80 (d, J = 8.4 Hz, 1H), 7.69 (s, 1H), 7.26 (d, J = 8.4 Hz, 1H), 7.20 (d, J = 8.3 Hz, 2H), 6.84 (d, J = 8.3 Hz, 2H), 4.69−4.65 (m, 1H), 4.43−4.37 (m, 1H), 4.33−4.27 (m, 1H), 3.78 (s, 3H), 3.29−3.25 (m, 1H) 3.15−3.09 (m, 1H), 1.27−1.23 (m, 3H). ^{13}C NMR (125.76 MHz, MeOH-d_4): δ 169.6, 169.2, 165.1, 158.5, 158.2, 131.7, 131.7, 128.3, 127.5, 125.9, 120.6, 120.5, 120.4, 117.1, 117.1, 68.6, 60.3, 56.7, 52.8, 37.4, 20.1. HRMS (ESI): m/z calcd for $C_{21}H_{26}N_4O_6$ + H$^+$ [M + H$^+$], 431.1925; found, 431.1931.

(*S*)-Benzyl 2-(4-Amino-3-((*S*)-2-amino-3-(4-hydroxyphenyl)-propanamido)benzamido)-3-(1*H*-indol-3-yl)propanoate (4p).

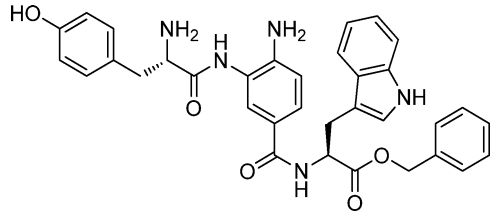

^{1}H NMR (500.13 MHz, MeOH-d_4): δ 7.55 (d, J = 7.9 Hz, 1H), 7.49 (s, 1H), 7.46−7.41 (m, 1H), 7.34 (d, J = 7.9 Hz, 1H), 7.30−7.25 (m, 3H), 7.19−7.14 (m, 2H), 7.14−7.05 (m, 3H), 7.03−6.97 (m, 2H), 6.78−6.71 (m, 3H), 5.07 (s, 2H), 4.93−4.87 (m, 1H), 3.82−3.76 (m, 1H), 3.43−3.37 (m, 1H), 3.35−3.33 (m, 1H), 3.05−2.97 (m, 1H), 2.95−2.86 (m, 1H). ^{13}C NMR (125.76 MHz, MeOH-d_4): δ 175.3, 173.8, 169.8, 157.5, 148.0, 138.1, 137.1, 131.6, 131.6, 129.5, 129.2, 129.2, 128.9, 128.8, 128.3, 127.7, 124.5, 123.1, 122.5, 122.2, 120.0, 119.2, 117.2, 116.7, 116.6, 116.6, 116.2, 112.5, 110.8, 68.2, 57.8, 55.6, 41.5, 28.6. HRMS (ESI): m/z calcd for $C_{34}H_{33}N_5O_5$ + H$^+$ [M + H$^+$], 592.2554; found, 592.2564.

(*S*)-2-(4-Amino-3-((*S*)-2-amino-3-(4-hydroxyphenyl)-propanamido)benzamido)-3-(1*H*-indol-3-yl)propanoic Acid (4p′).

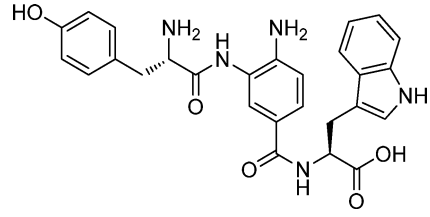

^{1}H NMR (500.13 MHz, MeOH-d_4): δ 7.71−7.50 (m, 3H), 7.39−7.29 (m, 2H), 7.20 (d, J = 8.4 Hz, 2H), 7.15 (s, 1H), 7.11−7.02 (m, 1H), 7.02−6.63 (m, 1H), 6.82 (d, J = 8.4 Hz, 2H), 4.95−4.90 (m, 1H), 4.42−4.30 (m, 1H), 3.55−3.40 (m, 1H), 3.40−3.32 (m, 1H), 3.25−3.15 (m, 1H), 3.14−3.04 (m, 1H). ^{13}C NMR (125.76 MHz, MeOH-d_4): δ 175.1, 169.9, 168.2, 158.4, 138.1, 133.9, 131.7, 131.7, 129.5, 128.8, 127.9, 127.0, 125.8, 124.5, 123.6, 122.4, 122.1, 119.9, 119.3, 117.1, 117.1, 112.4, 111.1, 56.5, 55.5, 37.8, 28.3. HRMS (ESI): m/z calcd for $C_{27}H_{27}N_5O_5$ + H$^+$ [M + H$^+$], 502.2085; found, 502.2080.

(*S*)-Benzyl 2-(4-Amino-3-((*S*)-2-amino-4-(4-(benzyloxy)-phenyl)butanamido) benzamido)-3-(1*H*-indol-3-yl)propanoate (4q).

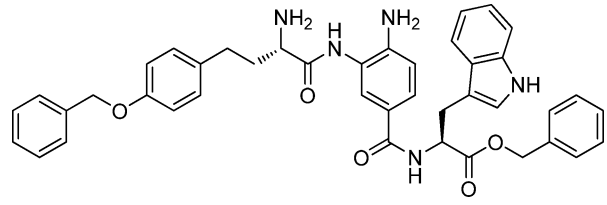

^{1}H NMR (500.13 MHz, MeOH-d_4): δ 7.75−7.63 (m, 2H), 7.55−7.48 (m, 1H), 7.41−7.11 (m, 14H), 7.07−6.86 (m, 5H), 5.06 (br.d, 2H), 4.99 (br.d, 2H), 4.95−4.89 (m, 1H), 4.38−4.22 (m, 1H), 3.49−3.35 (m, 1H), 3.36−3.30 (m, 1H), 2.87−2.67 (m, 2H), 2.41−2.31 (m, 1H), 2.29−2.19 (m, 1H). ^{13}C NMR (125.76 MHz, MeOH-d_4): δ 173.4, 170.1, 168.4, 158.9, 138.7, 138.0, 137.0, 134.9, 133.5, 132.8, 130.4, 130.4, 129.4, 129.4, 129.2, 129.2, 129.1, 129.1, 128.9, 128.8, 128.8, 128.7, 128.5, 128.5, 128.1, 127.0, 124.6, 123.2, 122.5, 119.9, 119.1, 116.2, 116.2, 112.4, 110.7, 71.0, 68.0, 55.9, 54.9, 34.6, 31.4, 28.3. HRMS (ESI): m/z calcd for $C_{42}H_{41}N_5O_5$ + H$^+$ [M + H$^+$], 696.3180; found, 696.3174.

DOI: 10.1021/jm501867s
J. Med. Chem. 2015, 58, 1524−1543

(*S*)-2-(4-Amino-3-((*S*)-2-amino-4-(4-hydroxyphenyl)-butanamido)benzamido)-3-(1*H*-indol-3-yl)propanoic Acid (4r).

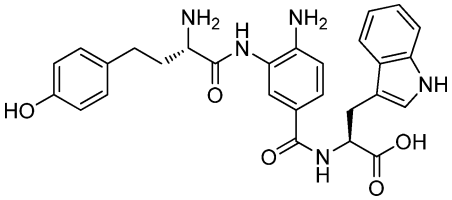

^{1}H NMR (500.13 MHz, MeOH-d_4): δ 7.65 (s, 1H), 7.59−7.39 (m, 3H), 7.29 (br.d, 1H), 7.14−6.91 (m, 5H), 6.74 (br.d, 2H), 4.71−4.49 (m, 1H), 4.30−4.04 (m, 1H), 3.46−3.38 (m, 1H), 3.30−3.28 (m, 1H), 2.76−2.64 (m, 2H), 2.32−2.22 (m, 1H), 2.23−2.13 (m, 1H). ^{13}C NMR (125.76 MHz, MeOH-d_4): δ 175.3, 169.8, 168.9, 157.1, 141.2, 138.0, 132.0, 130.3, 130.3, 128.4, 128.2, 127.6, 127.3, 125.5, 124.4, 122.4, 120.0, 119.8, 119.2, 116.5, 116.5, 112.3, 111.1, 55.3, 54.9, 35.0, 31.4, 28.3. HRMS (ESI): m/z calcd for $C_{28}H_{29}N_5O_5$ + H^+ [M + H^+], 516.2241; found, 516.2248.

(*S*)-Benzyl 2-(4-Amino-3-((*S*)-2-aminohexanamido)-benzamido)-3-methylbutanoate (4s).

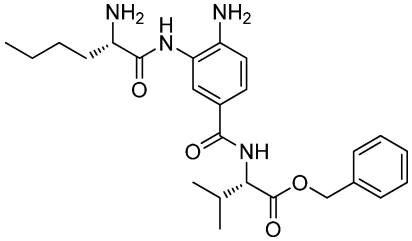

^{1}H NMR (500.13 MHz, MeOH-d_4): δ 7.85−7.77 (m, 2H), 7.40−7.29 (m, 6H), 5.27−5.13 (m, 2H), 4.50−4.46 (m, 1H), 4.24−4.18 (m, 1H), 2.31−2.22 (m, 1H), 2.15−2.04 (m, 1H), 2.03−1.93 (m, 1H), 1.57−1.42 (m, 4H), 1.04−0.95 (m, 9H). ^{13}C NMR (125.76 MHz, MeOH-d_4): δ 173.0, 170.4, 168.9, 151.1, 137.2, 129.6, 129.6, 129.5, 129.4, 128.6, 128.2, 128.2, 127.2, 127.2, 122.8, 67.9, 60.5, 55.1, 32.3, 31.6, 28.1, 23.4, 19.6, 19.2, 14.1. HRMS (ESI): m/z calcd for $C_{25}H_{34}N_4O_4$ + H^+ [M + H^+], 455.2653; found, 455.2653.

(*S*)-2-(4-Amino-3-((*S*)-2-aminohexanamido)benzamido)-3-methylbutanoic Acid (4s′).

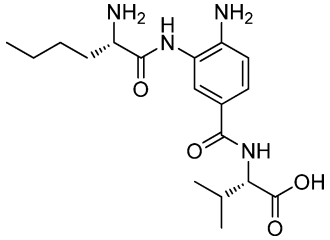

^{1}H NMR (500.13 MHz, MeOH-d_4): δ 7.91−7.86 (m, 2H), 7.56 (br.d, 1H), 4.50−4.46 (m, 1H), 4.28−4.22 (m, 1H), 2.34−2.25 (m, 1H), 2.16−2.06 (m, 1H), 2.03−1.96 (m, 1H), 1.58−1.42 (m, 4H), 1.08−1.02 (m, 6H), 1.02−0.96 (m, 3H). ^{13}C NMR (125.76 MHz, MeOH-d_4): δ 178.5, 171.0, 169.0, 147.6, 127.9, 127.3, 124.2, 122.3, 116.8, 61.7, 55.2, 33.1, 33.0, 28.3, 23.5, 20.2, 18.7, 14.1. HRMS (ESI): m/z calcd for $C_{18}H_{28}N_4O_4$ + H^+ [M + H^+], 365.2183; found, 365.2177.

(*S*)-Methyl 2-(4-Amino-3-((*S*)-2-aminohexanamido)-benzamido)-3-(4-hydroxyphenyl)propanoate (4t).

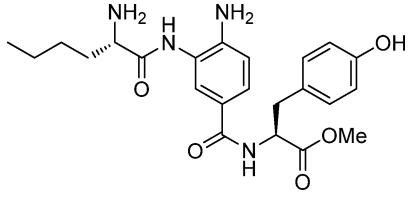

^{1}H NMR (500.13 MHz, MeOH-d_4): δ 7.83−7.72 (m, 2H), 7.51 (d, J = 8.3 Hz, 1H), 7.13−7.02 (m, 2H), 6.74−6.65 (m, 2H), 4.81−4.74 (m, 1H), 4.26−4.19 (m, 1H), 3.72 (s, 3H), 3.26−3.16 (m, 1H), 3.08−2.96 (m, 1H), 2.15−2.05 (m, 1H), 2.05−1.95 (m, 1H), 1.57−1.41 (m, 4H), 1.04−0.93 (m, 3H). ^{13}C NMR (125.76 MHz, MeOH-d_4): δ 174.7, 173.5, 170.7, 168.0, 157.4, 135.4, 131.2, 131.2, 131.0, 129.0, 127.9, 126.8, 125.0, 116.3, 116.3, 56.3, 55.1, 52.8, 37.3, 32.2, 28.1, 23.4, 14.1. HRMS (ESI): m/z calcd for $C_{23}H_{30}N_4O_5$ + H^+ [M + H^+], 443.2289; found, 443.2291.

(*S*)-Benzyl 2-(4-Amino-3-((*S*)-2-aminohexanamido)-benzamido)-3-(1*H*-indol-3-yl)propanoate (4u).

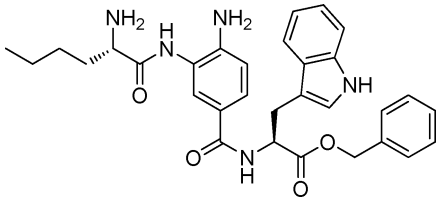

^{1}H NMR (500.13 MHz, MeOH-d_4): δ 7.78 (s, 1H), 7.70 (d, J = 7.8 Hz, 1H), 7.54 (d, J = 7.8 Hz, 1H), 7.40−7.30 (m, 2H), 7.30−7.25 (m, 3H), 7.22−7.16 (m, 2H), 7.11−7.06 (m, 1H), 7.04 (s, 1H), 7.01−6.95 (m, 1H), 5.09 (s, 2H), 4.24−4.16 (m, 1H), 3.48−3.38 (m, 1H), 3.38−3.32 (m, 2H), 2.12−2.04 (m, 1H), 2.03−1.93 (m, 1H), 1.56−1.39 (m, 4H), 1.02−0.94 (m, 3H). ^{13}C NMR (125.76 MHz, MeOH-d_4): δ 173.4, 170.4, 168.3, 138.1, 137.0, 133.3, 129.5, 129.5, 129.2, 129.2, 129.1, 129.1, 128.7, 128.0, 127.0, 124.5, 123.5, 123.4, 122.5, 119.9, 119.1, 112.4, 110.8, 68.0, 55.9, 55.1, 32.3, 28.3, 28.1, 23.4, 14.0. HRMS (ESI): m/z calcd for $C_{31}H_{35}N_5O_4$ + H^+ [M + H^+], 542.2762; found, 542.2759.

(*S*)-2-(4-Amino-3-((*S*)-2-aminohexanamido)benzamido)-3-(1*H*-indol-3-yl)propanoic Acid (4u′).

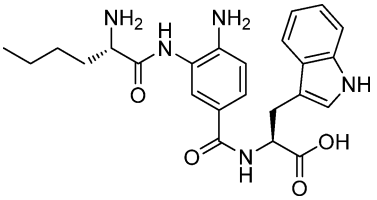

^{1}H NMR (500.13 MHz, MeOH-d_4): δ 7.76 (s, 1H), 7.70−7.64 (m, 1H), 7.58 (d, J = 7.8 Hz, 1H), 7.41−7.36 (m, 1H), 7.32 (d, J = 7.8 Hz, 1H), 7.15 (s, 1H), 7.09−7.03 (m, 1H), 7.00−6.93 (m, 1H), 4.93−4.90 (m, 1H), 4.26−4.18 (m, 1H), 3.53−3.44 (m, 1H), 3.37−3.32 (m, 1H), 2.14−2.04 (m, 1H), 2.02−1.94 (m, 1H), 1.55−1.40 (m, 4H), 1.02−0.92 (m, 3H). ^{13}C NMR (125.76 MHz, MeOH-d_4): δ 175.1, 170.5, 168.2, 138.0, 134.3, 133.2, 129.9, 128.8, 127.9, 126.9, 124.5, 124.0, 122.4, 119.8, 119.2, 112.3, 111.2, 55.5, 55.1, 32.2, 28.2, 28.1, 23.4, 14.1. HRMS (ESI): m/z calcd for $C_{24}H_{29}N_5O_4$ + H^+ [M + H^+], 452.2292; found, 452.2302.

(*S*)-Methyl 2-(4-Amino-3-((*S*)-2-aminohexanamido)-benzamido)-5-guanidinopentanoate (4v).

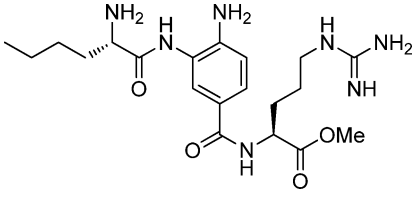

^{1}H NMR (500.13 MHz, MeOH-d_4): δ 8.00 (s, 1H), 7.98−7.94 (d, J = 7.8 Hz, 1H), 7.63 (d, J = 7.8 Hz, 1H), 4.65−4.58 (m, 1H), 4.33−4.27 (m, 1H), 3.75 (s, 3H), 2.17−1.92 (m, 4H), 1.85−1.62 (m, 3H), 1.60−1.40 (m, 5H), 1.04−0.92 (m, 3H). ^{13}C NMR (125.76 MHz, MeOH-d_4): δ 173.6, 170.6, 168.2, 158.6, 135.8, 131.5, 130.6, 128.1, 126.9, 125.6, 55.1, 54.2, 53.0, 42.0, 32.1, 29.2, 28.1, 26.6, 23.4, 14.1. HRMS (ESI): m/z calcd for $C_{20}H_{33}N_7O_4$ + H^+ [M + H^+], 436.2667; found, 436.2670.

DOI: 10.1021/jm501867s
J. Med. Chem. 2015, 58, 1524−1543

(*S*)-2-(4-Amino-3-((*S*)-2-amino-5-guanidinopentanamido)-benzamido)-3-methylbutanoic Acid (4w).

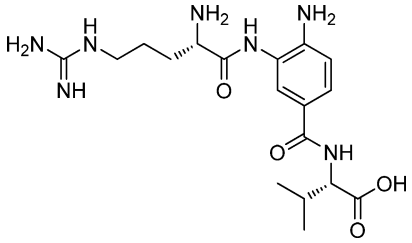

^{1}H NMR (500.13 MHz, MeOH-d_4): δ 7.91 (s, 1H), 7.83 (d, J = 8.3 Hz, 1H), 7.44−7.37 (m, 1H), 4.50−4.45 (m, 1H), 4.33−4.27 (m, 1H), 3.36−3.32 (m, 2H), 2.35−2.05 (m, 3H), 1.89−1.80 (m, 2H), 1.08−1.01 (m, 6H). ^{13}C NMR (125.76 MHz, MeOH-d_4): δ 174.9, 169.9, 169.1, 169.0, 158.7, 128.3, 128.1, 127.2, 122.5, 122.3, 60.0, 54.6, 41.8, 31.7, 29.7, 25.6, 19.7, 19.6. HRMS (ESI): m/z calcd for $C_{18}H_{29}N_7O_4$ + H$^+$ [M + H$^+$], 408.2354; found, 408.2354.

(*S*)-Methyl 2-(4-Amino-3-((*S*)-2-amino-5-guanidinopentanamido)benzamido)-3-(4-hydroxyphenyl)-propanoate (4x).

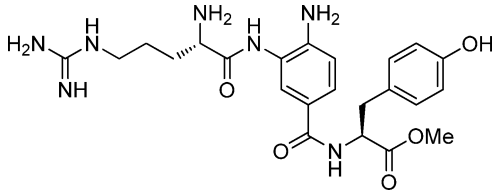

^{1}H NMR (500.13 MHz, MeOH-d_4): δ 7.90 (s, 1H), 7.76 (br.d, 1H), 7.60−7.47 (m, 1H), 7.08 (br.d, 2H), 6.70 (br.d, 2H), 4.82−4.74 (m, 1H), 4.39−4.29 (m, 1H), 3.72 (s, 3H), 3.40−3.27 (m, 2H), 3.26−3.14 (m, 1H), 3.13−2.97 (m, 1H), 2.25−2.06 (m, 2H), 1.92−1.76 (m, 2H). ^{13}C NMR (125.76 MHz, MeOH-d_4): δ 173.6, 170.0, 167.9, 158.6, 157.3, 151.2, 135.8, 131.2, 131.2, 129.0, 127.9, 126.8, 126.6, 125.3, 116.3, 116.3, 56.3, 54.6, 52.8, 41.8, 37.3, 29.6, 25.6. HRMS (ESI): m/z calcd for $C_{23}H_{31}N_7O_5$ + H$^+$ [M + H$^+$], 486.2459; found, 486.2466.

(*S*)-2-(4-Amino-3-((*S*)-2-amino-5-guanidinopentanamido)-benzamido)-3-(1*H*-indol-3-yl)propanoic Acid (4y).

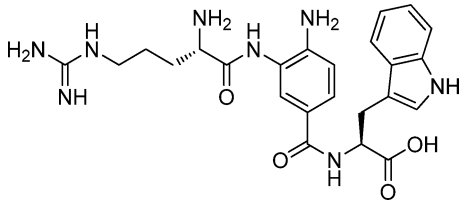

^{1}H NMR (500.13 MHz, MeOH-d_4): δ 7.83−7.55 (m, 2H), 7.39−7.21 (m, 2H), 7.20−6.88 (m, 4H), 4.32−4.24 (m, 1H), 3.93−3.81 (m, 1H), 3.69−3.49 (m, 2H), 3.34−3.40 (m, 2H), 2.17−2.00 (m, 2H), 1.88−1.76 (m, 2H). ^{13}C NMR (125.76 MHz, MeOH-d_4): δ 174.1, 170.5, 169.7, 168.6, 158.6, 138.0, 128.0, 127.2, 125.9, 124.5, 122.5, 121.6, 120.1, 119.8, 119.6, 119.1, 112.4, 110.9, 55.6, 54.5, 41.8, 29.7, 28.3, 25.6. HRMS (ESI): m/z calcd for $C_{24}H_{30}N_8O_4$ + H$^+$ [M + H$^+$], 495.2463; found, 495.2470.

(*S*)-Methyl 3-Amino-4-(2-amino-4-phenylbutanamido)-benzoate (6a).

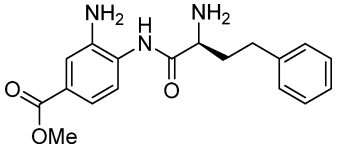

^{1}H NMR (500.13 MHz, MeOH-d_4): δ 8.17−8.06 (m, 2H), 7.67−7.58 (m, 1H), 7.35−7.27 (m, 4H), 7.25−7.18 (m, 1H), 4.45−4.36 (m, 1H), 3.94 (s, 3H), 2.90−2.80 (m, 2H), 2.48−2.37 (m, 1H), 2.36−2.26 (m, 1H). ^{13}C NMR (125.76 MHz, MeOH-d_4): δ 170.1, 166.4, 141.2, 135.6, 131.2, 131.1, 130.7, 129.7, 129.6, 129.4, 127.6, 127.1, 126.6, 126.5, 55.2, 53.1, 34.5, 32.3. HRMS (ESI): m/z calcd for $C_{18}H_{21}N_3O_3$ + H$^+$ [M + H$^+$], 328.1656; found, 328.1661.

(*S*)-Methyl 3-Amino-4-(2-amino-3-(4-(benzyloxy)phenyl)-propanamido)benzoate (6b).

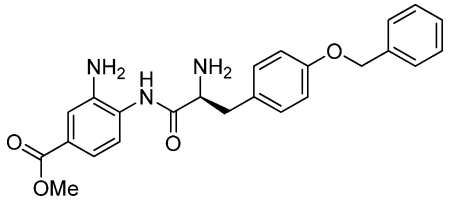

^{1}H NMR (500.13 MHz, MeOH-d_4): δ 7.90−7.85 (m, 1H), 7.79 (dd, J = 8.3, 1.7 Hz, 1H), 7.45−7.40 (m, 2H), 7.38−7.32 (m, 2H), 7.31−7.24 (m, 4H), 7.02 (d, J = 8.5 Hz, 3H), 5.18−4.99 (m, 2H), 4.45−4.27 (m, 1H), 3.95−3.85 (m, 3H), 3.37−3.32 (m, 1H), 3.20−3.10 (m, 1H). ^{13}C NMR (125.76 MHz, MeOH-d_4): δ 169.5, 167.0, 159.9, 143.4, 138.6, 133.1, 131.8, 131.8, 130.5, 129.5, 129.5, 128.9, 128.5, 128.4, 127.8, 127.5, 126.9, 124.3, 116.6, 116.6, 70.9, 56.4, 52.9, 37.7. HRMS (ESI): m/z calcd for $C_{24}H_{25}N_3O_4$ + H$^+$ [M + H$^+$], 420.1845; found, 420.1843.

(*S*)-Methyl 3-Amino-4-(2-amino-3-(4-hydroxyphenyl)-propanamido)benzoate (6c).

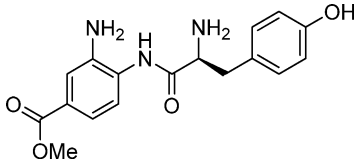

^{1}H NMR (500.13 MHz, MeOH-d_4): δ 7.63 (s, 1H), 7.50 (d, J = 8.2 Hz, 1H), 7.30−7.16 (m, 3H), 6.81 (d, J = 8.1 Hz, 2H), 4.40−4.30 (m, 1H), 3.95−3.85 (m, 3H), 3.30−3.07 (m, 2H). ^{13}C NMR (125.76 MHz, MeOH-d_4): δ 169.2, 167.8, 158.4, 143.4, 131.8, 131.8, 130.3, 126.8, 125.9, 123.7, 121.5, 121.3, 116.9, 116.9, 56.4, 52.7, 37.9. HRMS (ESI): m/z calcd for $C_{17}H_{19}N_3O_4$ + H$^+$ [M + H$^+$], 330.1448; found, 330.1457.

(*S*)-Methyl 3-Amino-4-(2-amino-4-methylpentanamido)-benzoate (6d).

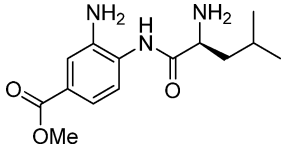

^{1}H NMR (500.13 MHz, MeOH-d_4): δ 8.15−8.04 (m, 2H), 7.62 (dd, J = 8.5, 3.2 Hz, 1H), 4.33−4.25 (m, 1H), 3.94 (s, 3H), 2.00−1.76 (m, 3H), 1.12−1.04 (m, 6H). ^{13}C NMR (125.76 MHz, MeOH-d_4): δ 170.8, 166.5, 135.4, 130.8, 130.8, 127.2, 126.4, 115.9, 53.7, 53.1, 41.3, 25.5, 23.4, 21.8. HRMS (ESI): m/z calcd for $C_{14}H_{21}N_3O_3$ + H$^+$ [M + H$^+$], 280.1656; found, 280.1650.

(*S*)-Methyl 3-Amino-4-(2-aminohexanoyl)benzoate (6e).

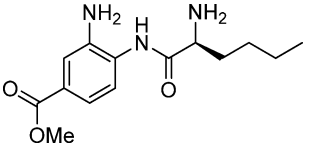

^{1}H NMR (500.13 MHz, MeOH-d_4): δ 8.10 (s, 1H), 8.04 (d, J = 8.4 Hz, 1H), 7.64 (d, J = 8.4 Hz, 1H), 4.31−4.25 (m, 1H), 3.94 (s, 3H), 2.16−1.96 (m, 2H), 1.58−1.39 (m, 4H), 1.02−0.94 (m, 3H). ^{13}C NMR (125.76 MHz, MeOH-d_4): δ 170.4, 166.5, 143.4, 135.3, 130.6, 128.0, 127.0, 126.2, 55.2, 53.1, 32.2, 28.1, 23.4, 14.1. HRMS (ESI): m/z calcd for $C_{14}H_{21}N_3O_3$ + H$^+$ [M + H$^+$], 280.1656; found, 280.1663.

(*S*)-Methyl 3-Amino-4-(2-amino-5-guanidinopentanamido)-benzoate (6f).

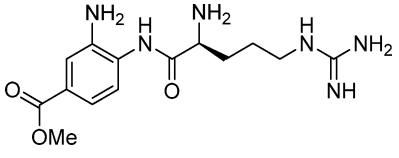

DOI: 10.1021/jm501867s
J. Med. Chem. 2015, 58, 1524−1543

^{1}H NMR (500.13 MHz, MeOH-d_4): δ 8.13 (s, 1H), 8.08 (dd, J = 8.4, 1.8 Hz, 1H), 7.71 (d, J = 8.4 Hz, 1H), 4.40−4.33 (m, 1H), 3.94 (s, 3H), 3.29−3.24 (m, 2H), 2.25−2.16 (m, 1H), 2.13−2.04 (m, 1H), 1.87−1.78 (m, 2H). ^{13}C NMR (125.76 MHz, MeOH-d_4): δ 167.9, 166.7, 158.3, 145.0, 131.6, 130.3, 126.8, 121.1, 118.6, 53.5, 52.8, 41.8, 29.3, 25.4. HRMS (ESI): m/z calcd for $C_{14}H_{22}N_6O_3$ + H^+ [M + H^+], 323.1826; found, 323.1822.

(*S*)-Methyl 6-Amino-2-(3,4-diaminobenzamido)hexanoate (9a).

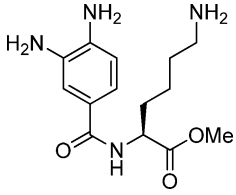

^{1}H NMR (500.13 MHz, MeOH-d_4): δ 7.80 (s, 1H), 7.75−7.70 (m, 1H), 7.04 (d, J = 8.5 Hz, 1H), 4.60−4.52 (m, 1H), 3.74 (s, 3H), 2.99−2.91 (m, 2H), 2.06−1.87 (m, 2H), 1.73 (m, 2H), 1.63−1.45 (m, 2H). ^{13}C NMR (125.76 MHz, MeOH-d_4): δ 174.1, 169.0, 142.9, 128.9, 125.8, 124.7, 120.1, 118.8, 54.2, 52.8, 40.5, 31.6, 28.0, 24.2. HRMS (ESI): m/z calcd for $C_{14}H_{22}N_4O_3$ + H^+ [M + H^+], 295.1765; found, 295.1765.

(*S*)-Methyl 2-(3,4-Diaminobenzamido)-3-(4-hydroxyphenyl)-propanoate (9b).

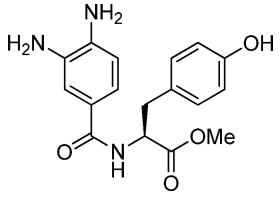

^{1}H NMR (500.13 MHz, MeOH-d_4): δ 7.68 (s, 1H), 7.60 (d, J = 8.3 Hz, 1H), 7.06 (d, J = 8.4 Hz, 2H), 7.02 (d, J = 8.3 Hz, 1H), 6.70 (d, J = 8.4 Hz, 2H), 4.76−4.68 (m, 1H), 3.70 (s, 3H), 3.21−3.12 (m, 1H), 3.07−2.97 (m, 1H). ^{13}C NMR (125.76 MHz, MeOH-d_4): δ 173.8, 168.7, 157.3, 142.5, 131.2, 131.2, 129.0, 128.7, 126.1, 124.6, 120.3, 119.0, 116.3, 116.3, 56.2, 52.7, 37.3. HRMS (ESI): m/z calcd for $C_{17}H_{19}N_3O_4$ + H^+ [M + H^+], 330.1448; found, 330.1447.

(*S*)-Benzyl 2-(3,4-Diaminobenzamido)-3-(1*H*-indol-3-yl)-propanoate (9c).

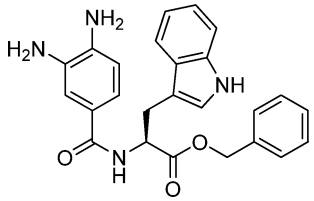

^{1}H NMR (500.13 MHz, MeOH-d_4): δ 7.63 (s, 1H), 7.58−7.46 (m, 2H), 7.38−7.23 (m, 4H), 7.20−7.11 (m, 2H), 7.11−6.88 (m, 4H), 5.09 (s, 2H), 4.92−4.85 (m, 1H), 3.47−3.34 (m, 2H). ^{13}C NMR (125.76 MHz, MeOH-d_4): δ 173.6, 168.8, 152.0, 143.4, 138.1, 137.1, 132.1, 129.5, 129.2, 129.2, 128.6, 126.9, 125.4, 125.4, 124.5, 122.5, 119.9, 119.2, 118.3, 117.6, 112.4, 110.8, 68.0, 55.8, 28.3. HRMS (ESI): m/z calcd for $C_{25}H_{24}N_4O_3$ + H^+ [M + H^+], 429.1921; found, 429.1930.

(*S*)-2-(3,4-Diaminobenzamido)-3-(1*H*-indol-3-yl)propanoic Acid (9c′).

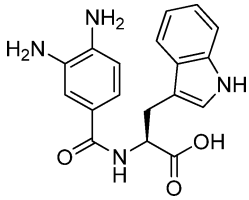

^{1}H NMR (500.13 MHz, MeOH-d_4): δ 7.63−7.53 (m, 2H), 7.49 (dd, J = 8.5, 2.0 Hz, 1H), 7.32 (d, J = 8.1 Hz, 1H), 7.12 (s, 1H), 7.09−7.04 (m, 1H), 6.99−6.94 (m, 1H), 6.92−6.87 (m, 1H), 4.92−4.85 (m, 1H), 3.53−3.40 (m, 2H). ^{13}C NMR (125.76 MHz, MeOH-d_4): δ 175.4, 168.7, 138.1, 131.9, 128.9, 128.1, 126.6, 124.4, 124.1, 122.4, 119.8, 119.3, 118.1, 117.5, 112.3, 111.2, 55.3, 28.3. HRMS (ESI): m/z calcd for $C_{18}H_{18}N_4O_3$ + H^+ [M + H^+], 339.1452; found, 339.1447.

(*S*)-Methyl 2-(3,4-Diaminobenzamido)-5-guanidinopentanoate (9d).

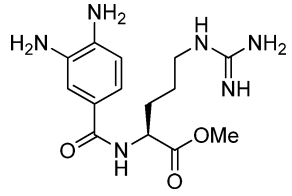

^{1}H NMR (500.13 MHz, MeOH-d_4): δ 7.77 (d, J = 1.9 Hz, 1H), 7.72 (dd, J = 8.5, 1.9 Hz 1H), 7.00 (d, J = 8.5 Hz, 1H), 4.62−4.53 (m, 1H), 3.73 (s, 3H), 3.28−3.18 (m, 2H), 2.10−1.85 (m, 2H), 1.84−1.63 (m, 2H). ^{13}C NMR (125.76 MHz, MeOH-d_4): δ 174.0, 169.1, 158.6, 143.6, 128.8, 125.2, 124.6, 119.7, 118.4, 53.9, 52.8, 42.0, 29.4, 26.6. HRMS (ESI): m/z calcd for $C_{14}H_{22}N_6O_3$ + H^+ [M + H^+], 323.1826; found, 323.1821.

(*S*)-Methyl 6-Amino-2-(3-amino-4-((*S*)-2-amino-4-phenylbutanamido)benzamido)hexanoate (10a).

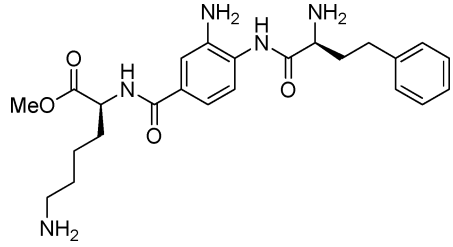

^{1}H NMR (500.13 MHz, MeOH-d_4): δ 8.05 (s, 1H), 8.00 (br.d, 1H), 7.62 (br.d, 1H), 7.33−7.16 (m, 5H), 4.64−4.56 (m, 1H), 4.46−4.40 (m, 1H), 3.75 (s, 3H), 3.03−2.91 (m, 2H), 2.92−2.84 (m, 2H), 2.52−2.40 (m, 1H), 2.38−2.28 (m, 1H), 2.08−1.80 (m, 2H), 1.82−1.70 (m, 2H), 1.66−1.46 (m, 2H). ^{13}C NMR (125.76 MHz, MeOH-d_4): δ 173.8, 170.1, 168.0, 141.3, 134.4, 129.7, 129.6, 129.6, 129.4, 129.4, 129.2, 127.6, 127.5, 127.1, 125.1, 55.2, 54.4, 52.9, 40.5, 34.4, 32.3, 31.6, 28.0, 24.2. HRMS (ESI): m/z calcd for $C_{24}H_{33}N_5O_4$ + H^+ [M + H^+], 456.2605; found, 456.2596.

(*S*)-Benzyl 2-(3-Amino-4-((*S*)-2-amino-4-phenylbutanamido)benzamido)-3-methylbutanoate (10b).

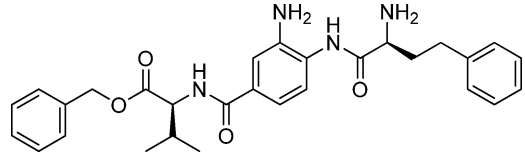

^{1}H NMR (500.13 MHz, MeOH-d_4): δ 7.90 (s, 1H), 7.85 (d, J = 8.3 Hz, 1H), 7.56 (d, J = 8.3 Hz, 1H), 7.40−7.25 (m, 9H), 7.23−7.15 (m, 1H), 5.25−5.20 (m, 1H), 5.18−5.13 (m, 1H), 4.52−4.47 (m, 1H), 4.44−4.38 (m, 1H), 2.90−2.83 (m, 2H), 2.48−2.38 (m, 1H), 2.37−2.23 (m, 2H), 1.04−0.96 (m, 6H). ^{13}C NMR (125.76 MHz, MeOH-d_4): δ 172.9, 170.0, 168.6, 141.3, 137.1, 134.6, 133.6, 130.2, 130.1, 129.8, 129.6, 129.5, 129.3, 128.8, 128.6, 128.1, 127.6, 127.4, 127.0, 126.9, 124.5, 67.9, 60.3, 55.1, 32.3, 31.8, 31.3, 19.6, 19.3. HRMS (ESI): m/z calcd for $C_{29}H_{34}N_4O_4$ + H^+ [M + H^+], 503.2653; found, 503.2649.

(*S*)-2-(3-Amino-4-((*S*)-2-amino-4-phenylbutanamido)-benzamido)-3-methylbutanoic Acid (10b′).

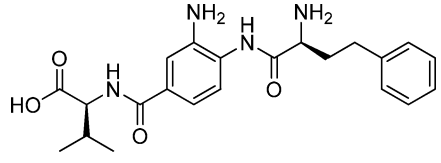

DOI: 10.1021/jm501867s
J. Med. Chem. 2015, 58, 1524−1543

^{1}H NMR (500.13 MHz, MeOH-d_4): δ 7.61 (s, 1H), 7.54 (d, J = 8.2 Hz, 1H), 7.45 (d, J = 8.2 Hz, 1H), 7.36−7.13 (m, 5H), 4.51−4.44 (m, 1H), 4.36−4.30 (m, 1H), 2.87−2.78 (m, 2H), 2.44−2.20 (m, 3H), 1.05 (d, J = 6.4 Hz, 6H). ^{13}C NMR (125.76 MHz, MeOH-d_4): δ 174.8, 169.5, 169.4, 141.3, 135.7, 134.7, 130.2, 129.7, 129.7, 129.4, 129.4, 127.5, 126.8, 123.1, 121.0, 59.9, 55.0, 34.7, 32.2, 31.7, 19.7, 18.9. HRMS (ESI): m/z calcd for $C_{22}H_{28}N_4O_4$ + H^+ [M + H^+], 413.2183; found, 413.2185.

(*S*)-Methyl 2-(3-Amino-4-((*S*)-2-amino-4-phenylbutanamido)benzamido)-3-(4-hydroxyphenyl)-propanoate (10c).

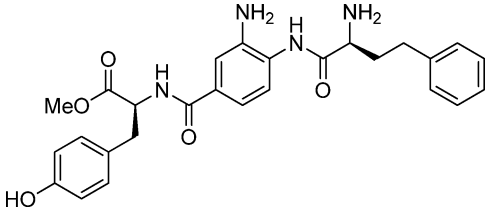

^{1}H NMR (500.13 MHz, MeOH-d_4): δ 7.89 (s, 1H), 7.84 (d, J = 8.3 Hz, 1H), 7.56 (d, J = 8.3 Hz, 1H), 7.31−7.28 (m, 4H), 7.24−7.15 (m, 1H), 7.08 (d, J = 8.4 Hz, 2H), 6.70 (d, J = 8.4 Hz, 2H), 4.82−4.76 (m, 1H), 4.43−4.32 (m, 1H), 3.72 (s, 3H), 3.24−3.15 (m, 1H), 3.08−3.00 (m 1H), 2.91−2.81 (m, 2H), 2.49−2.37 (m, 1H), 2.36−2.24 (m, 1H). ^{13}C NMR (125.76 MHz, MeOH-d_4): δ 173.6, 170.1, 167.6, 157.4, 141.2, 134.6, 134.5, 131.2, 131.2, 129.7, 129.7, 129.4, 129.4, 129.1, 128.9, 127.5, 127.1, 126.8, 125.2, 116.3, 116.3, 56.3, 55.1, 52.8, 37.3, 34.4, 32.3. HRMS (ESI): m/z calcd for $C_{27}H_{30}N_4O_5$ + H^+ [M + H^+], 491.2289; found, 491.2298.

(*S*)-Benzyl 2-(3-Amino-4-((*S*)-2-amino-4-phenylbutanamido)benzamido)-3-(1*H*-indol-3-yl)propanoate (10d).

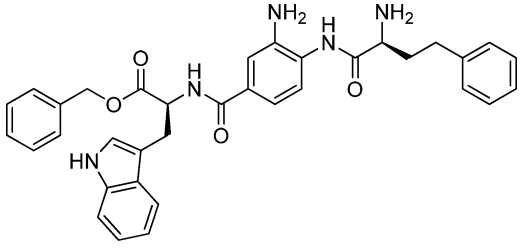

^{1}H NMR (500.13 MHz, MeOH-d_4): δ 7.75 (s, 1H), 7.66 (dd, J = 8.4, 1.7 Hz, 1H), 7.55 (d, J = 7.9 Hz, 1H), 7.46 (d, J = 8.4 Hz, 1H), 7.36−7.15 (m, 11H), 7.12−6.96 (m, 3H), 5.10 (s, 2H), 4.98−4.92 (m, 1H), 4.40−4.32 (m, 1H), 3.50−3.40 (m, 1H), 3.38−3.32 (m, 1H), 2.90−2.77 (m, 2H), 2.45−2.35 (m, 1H), 2.34−2.21 (m, 1H). ^{13}C NMR (125.76 MHz, MeOH-d_4): δ 173.4, 169.9, 168.2, 141.2, 138.1, 137.0, 134.5, 132.8, 130.3, 129.7, 129.7, 129.5, 129.5, 129.4, 129.4, 129.2, 129.2, 128.7, 127.6, 126.9, 126.7, 126.7, 124.5, 123.6, 122.5, 119.9, 119.1, 112.4, 110.7, 68.1, 55.9, 55.1, 34.5, 32.2, 28.3. HRMS (ESI): m/z calcd for $C_{35}H_{35}N_5O_4$ + H^+ [M + H^+], 590.2762; found, 590.2759.

(*S*)-Methyl 2-(3-Amino-4-((*S*)-2-amino-4-phenylbutanamido)benzamido)-5-guanidinopentanoate (10e).

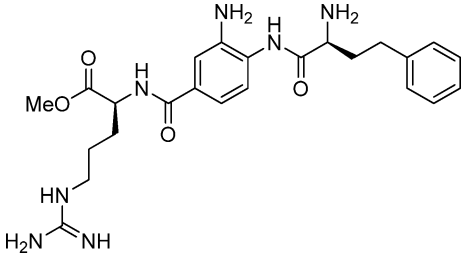

^{1}H NMR (500.13 MHz, MeOH-d_4): δ 8.07−7.91 (m, 2H), 7.58 (br.d, 1H), 7.34−7.16 (m, 5H), 4.67−4.58 (m, 1H), 4.43−4.35 (m, 1H), 3.75 (s, 3H), 3.29−3.20 (m, 2H), 2.91−2.81 (m, 2H), 2.47−2.24 (m, 2H), 2.13−1.89 (m, 2H), 1.89−1.66 (m, 2H). ^{13}C NMR (125.76 MHz, MeOH-d_4): δ 173.7, 171.9, 170.1, 168.1, 158.6, 154.2, 141.3, 134.3, 129.7, 129.6, 129.4, 127.6, 127.5, 127.1, 125.1, 124.8, 55.1, 54.2, 53.0, 41.9, 34.5, 32.3, 29.3, 26.6. HRMS (ESI): m/z calcd for $C_{24}H_{33}N_7O_4$ + H^+ [M + H^+], 484.2667; found, 484.2660.

(*S*)-Methyl 2-(3-Amino-4-((*S*)-2-amino-3-(4-(benzyloxy)-phenyl)propanamido) benzamido)-3-(4-hydroxyphenyl)-propanoate (10f).

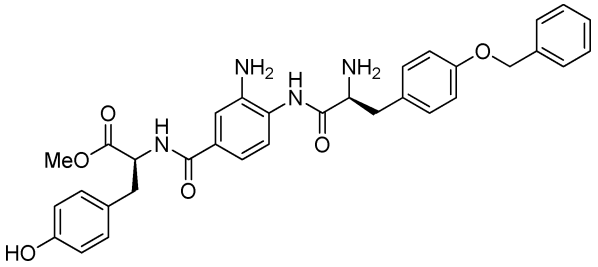

^{1}H NMR (500.13 MHz, MeOH-d_4): δ 7.74 (s, 1H), 7.69−7.65 (m, 1H), 7.47−7.41 (m, 2H), 7.39−7.34 (m, 2H), 7.31−7.26 (m, 3H), 7.24−7.20 (m, 1H), 7.09−7.00 (m, 4H), 6.73−6.68 (m, 2H), 5.13−5.10 (m, 2H), 4.82−4.77 (m, 1H), 4.42−4.36 (m, 1H), 3.74−3.71 (m, 3H), 3.37−3.32 (m, 1H), 3.24−3.14 (m, 2H), 3.08−2.97 (m, 1H). ^{13}C NMR (125.76 MHz, MeOH-d_4): δ 173.6, 169.6, 168.0, 165.8, 159.9, 157.4, 138.6, 135.8, 134.8, 131.8, 131.8, 131.2, 131.2, 129.9, 129.6, 128.9, 128.9, 128.5, 127.4, 127.0, 127.0, 123.7, 121.7, 116.8, 116.8, 116.3, 116.3, 71.0, 56.5, 56.2, 52.8, 37.7, 37.4. HRMS (ESI): m/z calcd for $C_{33}H_{34}N_4O_6$ + H^+ [M + H^+], 583.2511; found, 583.2504.

(*S*)-Methyl 2-(3-Amino-4-((*S*)-2-amino-3-(4-hydroxyphenyl)-propanamido) benzamido)-3-(4-hydroxyphenyl)propanoate (10g).

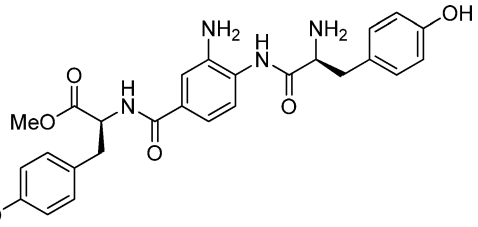

^{1}H NMR (500.13 MHz, MeOH-d_4): δ 7.79 (br.s, 1H), 7.74 (br.d, 1H), 7.27 (br.d, 1H), 7.19 (d, J = 8.3 Hz, 2H), 7.07 (br.d, 2H), 6.82 (d, J = 8.3 Hz, 2H), 6.69 (br.d, 2H), 4.82−4.76 (m, 1H), 4.41−4.35 (m, 1H), 3.73 (s, 3H), 3.28−3.09 (m, 3H), 3.06−2.99 (m, 1H). ^{13}C NMR (125.76 MHz, MeOH-d_4): δ 173.6, 169.8, 167.8, 158.4, 157.4, 134.8, 133.4, 131.8, 131.8, 131.2, 131.2, 128.9, 127.8, 127.7, 127.1, 125.8, 124.2, 117.0, 117.0, 116.3, 116.3, 56.6, 56.3, 52.8, 37.7, 37.4. HRMS (ESI): m/z calcd for $C_{26}H_{28}N_4O_6$ + H^+ [M + H^+], 493.2082; found, 493.2082.

(*S*)-Benzyl 2-(3-Amino-4-((*S*)-2-amino-3-(4-(benzyloxy)-phenyl)propanamido)benzamido)-3-(1*H*-indol-3-yl)-propanoate (10h).

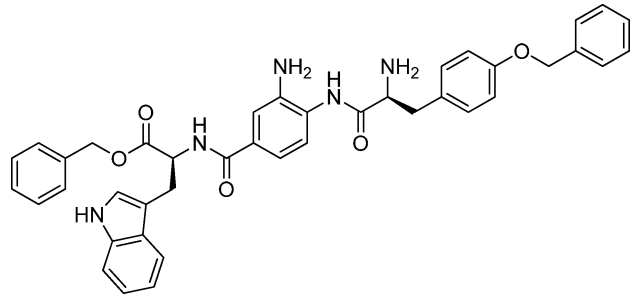

^{1}H NMR (500.13 MHz, MeOH-d_4): δ 7.72 (s, 1H), 7.61 (br.d, 1H), 7.55 (d, J = 7.9 Hz, 1H), 7.46−7.39 (m, 2H), 7.38−7.32 (m, 3H), 7.31−7.23 (m, 6H), 7.22−7.16 (m, 3H), 7.11−6.95 (m, 5H), 5.14−5.06 (m, 4H), 4.98−4.92 (m, 1H), 4.38−4.33 (m, 1H), 3.49−3.40 (m, 1H), 3.38−3.32 (m, 2H), 3.20−3.10 (m, 1H). ^{13}C NMR (125.76 MHz, MeOH-d_4): δ 173.3, 169.7, 167.8, 159.9, 138.6, 138.0, 137.0, 134.6, 131.8, 131.8, 131.6, 129.5, 129.5, 129.4, 129.4, 129.2, 129.2, 128.9, 128.7, 128.5, 128.5, 128.3, 128.1, 127.4, 127.0, 124.6, 124.6,

DOI: 10.1021/jm501867s
J. Med. Chem. 2015, 58, 1524−1543

122.5, 119.9, 119.1, 116.6, 116.6, 116.5, 112.5, 110.7, 70.9, 68.1, 56.5, 55.9, 37.6, 28.3. HRMS (ESI): m/z calcd for $C_{41}H_{39}N_5O_5 + H^+$ [M + H^+], 682.3024; found, 682.3020.

(*S*)-2-(3-Amino-4-((*S*)-2-amino-3-(4-hydroxyphenyl)-propanamido)benzamido)-3-(1*H*-indol-3-yl)propanoic Acid (10h′).

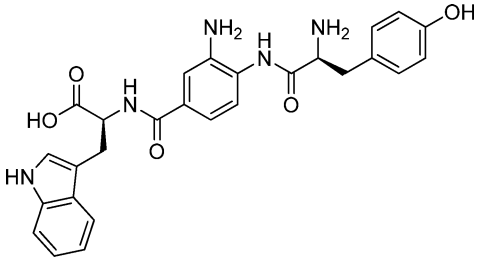

^{1}H NMR (500.13 MHz, MeOH-d_4): δ 7.58 (br.d, 1H), 7.46−6.90 (m, 9H), 6.84−6.76 (m, 2H), 4.92−4.88 (m, 1H), 4.31−4.21 (m, 1H), 3.50−3.42 (m, 1H), 3.25−3.07 (m, 3H). ^{13}C NMR (125.76 MHz, MeOH-d_4): δ 175.3, 169.8, 168.7, 158.4, 143.1, 138.1, 134.4, 131.8, 129.5, 128.9, 128.5, 126.7, 126.0, 124.4, 122.4, 119.9, 119.3, 117.5, 116.9, 116.9, 116.7, 112.3, 111.1, 56.3, 55.2, 38.1, 28.3. HRMS (ESI): m/z calcd for $C_{27}H_{27}N_5O_5 + H^+$ [M + H^+], 502.2085; found, 502.2088.

(*S*)-Methyl 6-Amino-2-(3-amino-4-((*S*)-2-amino-3-(4-hydroxyphenyl)propanamido)benzamido)hexanoate (10i).

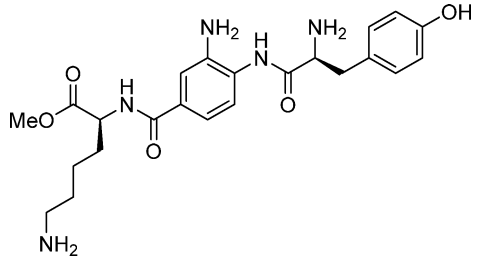

^{1}H NMR (500.13 MHz, MeOH-d_4): δ 7.86 (s, 1H), 7.79 (br.d, 1H), 7.30 (br.d, 1H), 7.20 (br.d, 2H), 6.81 (br.d, 2H), 4.63−4.55 (m, 1H), 4.43−4.36 (m, 1H), 3.75 (s, 3H), 3.38−3.32 (m, 1H), 3.23−3.10 (m, 1H), 3.00−2.90 (m, 2H), 2.11−1.86 (m, 2H), 1.81−1.67 (m, 2H), 1.59−1.50 (m, 2H). ^{13}C NMR (125.76 MHz, MeOH-d_4): δ 173.9, 169.6, 168.5, 158.3, 134.4, 132.6, 131.8, 131.8, 130.8, 127.1, 126.7, 125.8, 123.4, 116.9, 116.9, 56.5, 54.4, 52.9, 40.6, 37.7, 31.6, 28.0, 24.2. HRMS (ESI): m/z calcd for $C_{23}H_{31}N_5O_5 + H^+$ [M + H^+], 458.2398; found, 458.2407.

(*S*)-Benzyl 2-(3-Amino-4-((*S*)-2-amino-4-(4-(benzyloxy)-phenyl)butanamido) benzamido)-3-(1*H*-indol-3-yl)propanoate (10j).

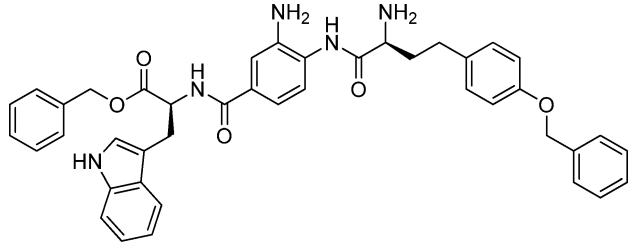

^{1}H NMR (500.13 MHz, MeOH-d_4): δ 7.62 (br.s, 1H), 7.58−7.49 (m, 2H), 7.44−7.23 (m, 10H), 7.23−6.89 (m, 9H), 5.12−5.01 (m, 4H), 4.98−4.90 (m, 1H), 4.31−4.23 (m, 1H), 3.48−3.39 (m, 1H), 3.27−3.20 (m, 1H), 2.82−2.71 (m, 2H), 2.38−2.29 (m, 1H), 2.28−2.19 (m, 1H). ^{13}C NMR (125.76 MHz, MeOH-d_4): δ 173.4, 169.7, 168.6, 159.0, 138.8, 138.1, 137.1, 134.6, 133.5, 132.3, 131.3, 130.4, 130.4, 130.4, 129.5, 129.5, 129.3, 129.2, 128.8, 128.8, 128.5, 126.8, 124.5, 124.5, 122.5, 122.4, 122.0, 119.9, 119.2, 119.2, 116.3, 116.3, 112.4, 110.8, 109.7, 71.1, 68.1, 55.9, 55.0, 34.7, 31.3, 28.3. HRMS (ESI): m/z calcd for $C_{42}H_{41}N_5O_5 + H^+$ [M + H^+], 696.3175; found, 696.3180.

(*S*)-2-(3-Amino-4-((*S*)-2-amino-4-(4-hydroxyphenyl)-butanamido)benzamido)-3-(1*H*-indol-3-yl)propanoic Acid (10j′).

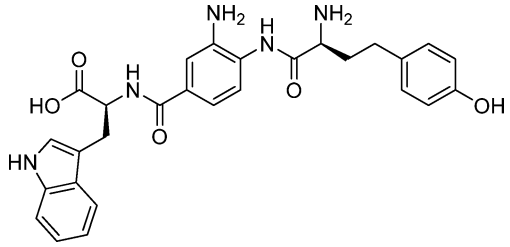

^{1}H NMR (500.13 MHz, MeOH-d_4): δ 7.90 (s, 1H), 7.84 (br.d, 1H), 7.58−7.50 (m, 2H), 7.33 (d, J = 8.3 Hz, 1H), 7.14−6.96 (m, 4H), 6.76−6.69 (m, 3H), 4.93−4.91 (m, 1H), 4.40−4.31 (m, 1H), 3.38−3.32 (m, 2H), 2.81−2.70 (m, 2H), 2.43−2.32 (m, 1H), 2.31−2.20 (m, 1H). ^{13}C NMR (125.76 MHz, MeOH-d_4): δ 175.0, 170.3, 167.6, 157.1, 138.1, 134.7, 131.9, 130.4, 130.4, 129.5, 127.1, 125.5, 125.4, 124.5, 122.5, 122.4, 119.9, 119.2, 119.1, 116.4, 116.4, 112.4, 112.4, 55.7, 55.1, 34.7, 31.4, 28.2. HRMS (ESI): m/z calcd for $C_{28}H_{29}N_5O_5 + H^+$ [M + H^+], 516.2241; found, 516.2249.

(*S*)-Benzyl 2-(3-Amino-4-((*S*)-2-amino-4-methylpentanamido)benzamido)-3-(1*H*-indol-3-yl)propanoate (10k).

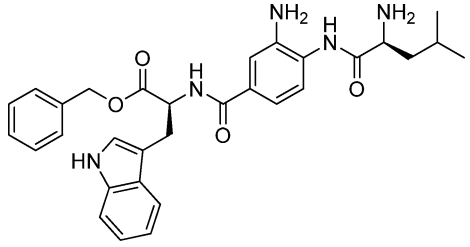

^{1}H NMR (500.13 MHz, MeOH-d_4): δ 7.78 (s, 1H), 7.72 (br.d, 1H), 7.54 (d, J = 7.7 Hz, 1H), 7.50 (d, J = 8.3 Hz, 1H), 7.36−7.25 (m, 4H), 7.22−7.16 (m, 2H), 7.11−6.96 (m, 3H), 5.13−5.06 (s, 2H), 4.98−4.92 (m, 1H), 4.30−4.21 (m, 1H), 3.48−3.40 (m, 1H), 3.39−3.33 (m, 1H), 1.96−1.76 (m, 3H), 1.11−1.04 (br.s, 6H). ^{13}C NMR (125.76 MHz, MeOH-d_4): δ 173.3, 170.7, 168.1, 138.1, 137.1, 134.8, 133.2, 129.8, 129.5, 129.4, 129.3, 129.2, 128.8, 128.2, 127.3, 127.0, 124.5, 124.0, 122.5, 119.9, 119.2, 112.4, 110.8, 68.1, 55.9, 53.7, 41.4, 28.3, 25.5, 23.4, 21.9. HRMS (ESI): m/z calcd for $C_{31}H_{35}N_5O_4 + H^+$ [M + H^+], 542.2762; found, 542.2761.

(*S*)-Methyl 6-Amino-2-(3-amino-4-((*S*)-2-amino-4-methylpentanamido)benzamido)hexanoate (10l).

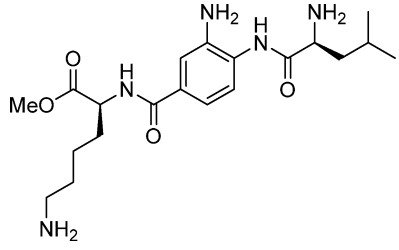

^{1}H NMR (500.13 MHz, MeOH-d_4): δ 7.99−7.93 (m, 2H), 7.60 (d, J = 8.4 Hz, 1H), 4.65−4.57 (m, 1H), 4.32−4.23 (m, 1H), 3.76 (s, 3H), 3.00−2.90 (m, 2H), 2.11−1.81 (m, 5H), 1.79−1.68 (m, 2H), 1.67−1.46 (m, 2H), 1.13−1.04 (m, 6H). ^{13}C NMR (125.76 MHz, MeOH-d_4): δ 173.9, 170.8, 168.2, 134.6, 133.9, 128.4, 128.3, 127.1, 124.6, 54.4, 53.6, 52.9, 41.4, 40.5, 31.7, 28.1, 25.5, 24.2, 23.4, 21.8. HRMS (ESI): m/z calcd for $C_{20}H_{33}N_5O_4 + H^+$ [M + H^+], 408.2605; found, 408.2604.

DOI: 10.1021/jm501867s
J. Med. Chem. 2015, 58, 1524−1543

(*S*)-Benzyl 2-(3-Amino-4-((*S*)-2-aminohexanamido)-benzamido)-3-methylbutanoate (10m).

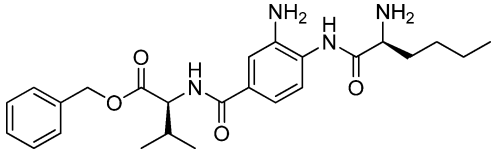

^{1}H NMR (500.13 MHz, MeOH-d_4): δ 7.92−7.68 (m, 2H), 7.58 (d, J = 8.4 Hz, 1H), 7.42−7.28 (m, 5H), 5.26−5.14 (m, 2H), 4.52−4.47 (m, 1H), 4.27−4.22 (m, 1H), 2.35−2.20 (m, 1H), 2.14−2.06 (m, 1H), 2.05−1.96 (m, 1H), 1.56−1.41 (m, 4H), 1.05−0.94 (m, 9H). ^{13}C NMR (125.76 MHz, MeOH-d_4): δ 172.9, 170,4, 168.5, 137.2, 134.8, 133.9, 129.6, 129.6, 129.5, 129.5, 129.4, 129.4, 128.4, 126.9, 124.7, 67.9, 60.5, 55.2, 32.3, 31.6, 28.1, 23.4, 19.6, 19.2, 14.1. HRMS (ESI): m/z calcd for $C_{25}H_{34}N_4O_4$ + H^+ [M + H^+], 455.2653; found, 455.2653.

(*S*)-2-(3-Amino-4-((*S*)-2-aminohexanamido)benzamido)-3-methylbutanoic Acid (10m′).

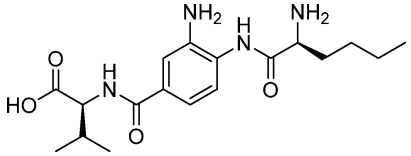

^{1}H NMR (500.13 MHz, MeOH-d_4): δ 7.99−7.92 (m, 2H), 7.60 (d, J = 7.9 Hz, 1H), 4.51−4.46 (m, 1H), 4.29−4.22 (m, 1H), 2.34−2.24 (m, 1H), 2.15−2.06 (m, 1H), 2.05−1.95 (m, 1H), 1.58−1.35 (m, 4H), 1.08−1.03 (m, 6H), 1.02−0.96 (m, 3H). ^{13}C NMR (125.76 MHz, MeOH-d_4): δ 174.7, 170.5, 168.2, 135.0, 134.3, 129.0, 127.3, 127.0, 125.1, 60.1, 55.2, 32.2, 31.6, 28.1, 23.4, 19.7, 18.9, 14.1. HRMS (ESI): m/z calcd for $C_{18}H_{28}N_4O_4$ + H^+ [M + H^+], 365.2183; found, 365.2177.

(*S*)-Methyl 2-(3-Amino-4-((*S*)-2-aminohexanamido)-benzamido)-3-(4-hydroxyphenyl)propanoate (10n).

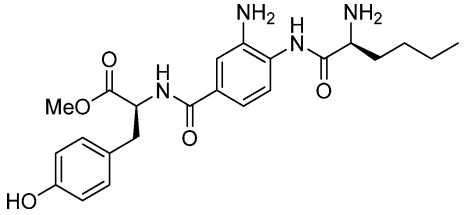

^{1}H NMR (500.13 MHz, MeOH-d_4): δ 7.86−7.76 (m, 2H), 7.56 (br.d, 1H), 7.11−7.04 (m, 2H), 6.72−6.67 (m, 2H), 4.82−4.75 (m, 1H), 4.27−4.18 (m, 1H), 3.73 (s, 3H), 3.24−3.16 (m, 1H), 3.07−2.97 (m, 1H), 2.15−2.04 (m, 1H), 2.02−1.93 (m, 1H), 1.58−1.42 (m, 4H), 1.03−0.94 (m, 3H). ^{13}C NMR (125.76 MHz, MeOH-d_4): δ 173.6, 170.4, 167.8, 157.4, 134.7, 134.0, 131.2, 131.2, 128.9, 128.4, 126.9, 124.7, 116.3, 116.3, 116.2, 56.3, 55.2, 52.8, 37.4, 32.2, 28.1, 23.4, 14.1. HRMS (ESI): m/z calcd for $C_{23}H_{30}N_4O_5$ + H^+ [M + H^+], 443.2289; found, 443.2288.

(*S*)-Benzyl 2-(3-Amino-4-((*S*)-2-aminohexanamido)-benzamido)-3-(1*H*-indol-3-yl)propanoate (10o).

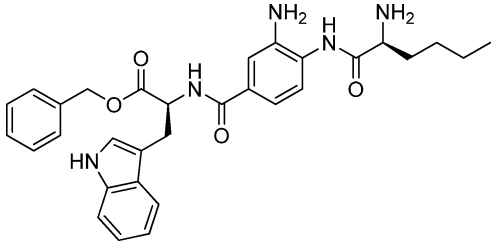

^{1}H NMR (500.13 MHz, MeOH-d_4): δ 7.77 (s, 1H), 7.70 (br.d, 1H), 7.55 (d, J = 7.8 Hz, 1H), 7.50 (d, J = 8.3 Hz, 1H), 7.36−7.26 (m, 4H), 7.23−7.16 (m, 2H), 7.12−6.96 (m, 3H), 5.11 (s, 2H), 4.98−4.92 (m, 1H), 4.25−4.18 (m, 1H), 3.48−3.40 (m, 1H), 3.37−3.32 (m, 1H), 1.55−1.37 (m, 6H), 1.02−0.94 (m, 3H). ^{13}C NMR (125.76 MHz, MeOH-d_4): δ 173.4, 170.3, 168.1, 138.1, 137.1, 134.6, 134.5, 133.1, 129.5, 129.5, 129.3, 129.2, 128.8, 127.1, 126.8, 124.5, 123.9, 122.5, 119.9, 119.2, 112.4, 110.8, 110.7, 68.1, 55.9, 55.2, 32.3, 28.3, 28.1, 23.4, 14.1. HRMS (ESI): m/z calcd for $C_{31}H_{35}N_5O_4$ + H^+ [M + H^+], 542.2762; found, 542.2760.

(*S*)-2-(3-Amino-4-((*S*)-2-aminohexanamido)benzamido)-3-(1*H*-indol-3-yl)propanoic Acid (10o′).

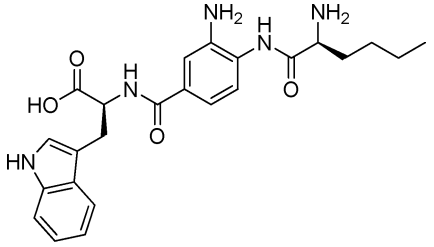

^{1}H NMR (500.13 MHz, MeOH-d_4): δ 7.81 (s, 1H), 7.75 (br.d, 1H), 7.58 (d, J = 7.9 Hz, 1H), 7.51 (d, J = 8.3 Hz, 1H), 7.32 (d, J = 8.0 Hz, 1H), 7.14 (s, 1H), 7.10−7.04 (m, 1H), 7.02−6.94 (m, 1H), 4.95−4.91 (m, 1H), 4.26−4.18 (m, 1H), 3.56−3.39 (m, 2H), 2.10−1.90 (m, 2H), 1.56−1.36 (m, 4H), 1.03−0.92 (m, 3H). ^{13}C NMR (125.76 MHz, MeOH-d_4): δ 170.4, 167.8, 159.6, 138.1, 133.8, 128.3, 128.1, 126.9, 124.5, 124.4, 122.5, 122.4, 119.9, 119.8, 119.2, 119.1, 112.3, 61.3, 55.2, 32.3, 28.2, 28.1, 23.4, 14.1. HRMS (ESI): m/z calcd for $C_{24}H_{29}N_5O_4$ + H^+ [M + H^+], 452.2292; found, 452.2297.

(*S*)-Methyl 6-Amino-2-(3-amino-4-((*S*)-2-aminohexanamido)benzamido)hexanoate (10p).

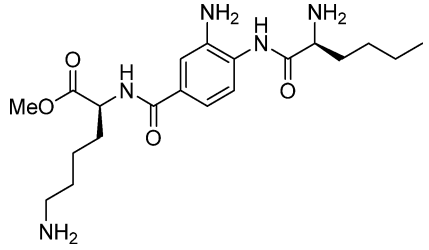

^{1}H NMR (500.13 MHz, MeOH-d_4): δ 8.07−7.94 (m, 2H), 7.62 (d, J = 8.3 Hz, 1H), 4.63−4.57 (m, 1H), 4.32−4.22 (m, 1H), 3.75 (s, 3H), 3.00−2.90 (m, 2H), 2.17−1.90 (m, 4H), 1.91−1.66 (m, 2H), 1.65−1.32 (m, 6H), 1.06−0.83 (m, 3H). ^{13}C NMR (125.76 MHz, MeOH-d_4): δ 173.9, 170.4, 168.1, 134.4, 134.3, 128.9, 127.5, 127.0, 125.0, 55.2, 54.4, 52.9, 40.5, 32.2, 31.6, 28.1, 28.0, 24.2, 23.4, 14.1. HRMS (ESI): m/z calcd for $C_{20}H_{33}N_5O_4$ + H^+ [M + H^+], 408.2605; found, 408.2608.

(*S*)-Methyl 2-(3-Amino-4-((*S*)-2-amino-5-guanidinopentanamido)benzamido)-3-(4-hydroxyphenyl)-propanoate (10q).

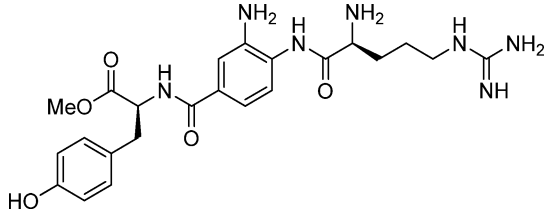

^{1}H NMR (500.13 MHz, MeOH-d_4): δ 7.95−7.82 (m, 2H), 7.67 (d, J = 8.4 Hz, 1H), 7.09 (d, J = 8.0 Hz, 2H), 6.71 (d, J = 8.0 Hz, 2H), 4.82−4.74 (m, 1H), 4.40−4.28 (m, 1H), 3.73 (s, 3H), 3.38−3.32 (m, 2H), 3.23−3.15 (m, 1H), 3.09−2.99 (m, 1H), 2.30−2.17 (m, 1H), 2.16−2.05 (m, 1H), 1.95−1.76 (m, 2H). ^{13}C NMR (125.76 MHz, MeOH-d_4): δ 173.6, 169.9, 167.6, 158.6, 157.4, 134.7, 134.6, 131.2, 131.2, 129.4, 128.9, 127.1, 126.4, 125.4, 116.3, 116.3, 56.3, 54.7, 52.8, 41.8, 37.3, 29.6, 25.7. HRMS (ESI): m/z calcd for $C_{23}H_{31}N_7O_5$ + H^+ [M + H^+], 486.2459; found, 484.2458.

DOI: 10.1021/jm501867s
J. Med. Chem. 2015, 58, 1524−1543

(*S*)-2-(3-Amino-4-((*S*)-2-amino-5-guanidinopentanamido)-benzamido)-3-(1*H*-indol-3-yl) propanoic Acid (10r).

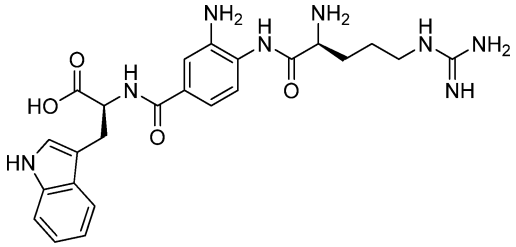

^{1}H NMR (500.13 MHz, MeOH-d_4): δ 7.80 (s, 1H), 7.74 (d, J = 8.1 Hz, 1H), 7.63−7.56 (m, 2H), 7.32 (d, J = 8.1 Hz, 1H), 7.14 (s, 1H), 7.10−7.05 (m, 1H), 7.01−6.94 (m, 1H), 4.97−4.89 (m, 1H), 4.37−4.26 (m, 1H), 3.37−3.32 (m, 2H), 3.25−3.20 (m, 2H), 2.28−2.03 (m, 2H), 1.91−1.79 (m, 2H). ^{13}C NMR (125.76 MHz, MeOH-d_4): δ 175.0, 169.9, 167.8, 158.7, 138.1, 133.8, 128.06, 126.9, 124.6, 124.4, 122.5, 122.4, 119.9, 119.2, 119.1, 112.4, 112.3, 111.2, 64.9, 54.7, 41.8, 29.7, 28.3, 25.7. HRMS (ESI): m/z calcd for $C_{24}H_{30}N_8O_4$ + H^+ [M + H^+], 495.2463; found, 495.2468.

(*S*)-Methyl 6-Amino-2-(3-amino-4-((*S*)-2-amino-5-guanidinopentanamido)benzamido)hexanoate (10s).

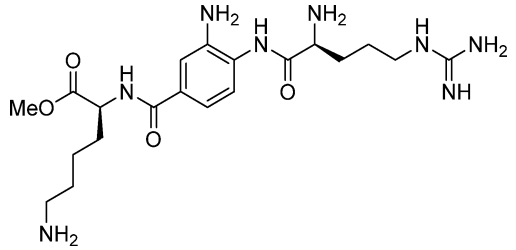

^{1}H NMR (500.13 MHz, MeOH-d_4): δ 8.02−7.94 (m, 2H), 7.70 (br.d, 1H), 4.65−4.58 (m, 1H), 4.37−4.30 (m, 1H), 3.76 (s, 3H), 3.37−3.32 (m, 2H), 2.99−2.91 (m, 2H), 2.14−1.90 (m, 4H), 1.89−1.69 (m, 4H), 1.65−1.48 (m, 2H). ^{13}C NMR (125.76 MHz, MeOH-d_4): δ 173.9, 169.9, 168.1, 158.8, 134.5, 134.1, 128.6, 127.1, 126.9, 124.9, 54.7, 54.4, 52.9, 41.9, 40.6, 31.7, 29.7, 28.1, 25.7, 24.1. HRMS (ESI): m/z calcd for $C_{20}H_{34}N_8O_4$ + H^+ [M + H^+], 451.2776; found, 451.2778.

Protein Expression and Purification. The expression and purification of recombinant human endoplasmic reticulum aminopeptidase 1 (ERAP1), endoplasmic reticulum aminopeptidase 2 (ERAP2), and insulin-regulated aminopeptidase (IRAP) have been described before.[23,24] Recombinant baculovirus containing each ERAP1 variant was produced in sf9 cells according to the manufacturer's instructions (Bac-to-Bac baculovirus expression system, Invitrogen). Recombinant proteins were expressed in Hi5 cells after infection with the appropriate recombinant baculovirus and purified as previously described.[24] Proteins were aliquoted in and stored in a buffer containing 10 mM Hepes, pH 7, 100 mM NaCl, and 10% glycerol at −80 °C, until needed.

Enzymatic Assays. The enzymatic activity of the enzymes was calculated by following the time-dependent increase in fluorescence at 460 nm (excitation was at 380 nm) of the fluorigenic substrates L-leucine-7-amido-4-methyl coumarin (L-AMC; Sigma) for ERAP1 and IRAP and L-arginyl-7-amido-4-methyl coumarin (R-AMC; Sigma) for ERAP2. All measurements were performed on a TECAN infinite M200 microplate fluorescence reader. For evaluation of the effect of the compound on activity, 30 nM ERAP1, 6 nM ERAP2, or 6 nM IRAP was added to each well along with 50 μM substrate and varied concentrations of compound. In all cases, the enzyme concentration used was significantly less than the calculated IC_{50} values for the inhibitors in order to avoid ligand depletion artifacts. The reaction was followed for 5−10 min, and activity was calculated by measuring the slope of the time course. For calculation of the in vitro IC_{50} values, experimental data were fit to the following equation using the GraphPad Prism software package

$$Y = \text{bottom} + (\text{top} - \text{bottom})/(1 + 10^{((\text{Log IC}_{50} - X) \times \text{Hill Slope})})$$

where Y is the enzymatic activity and X is the inhibitor concentration.

Phagocytosis Assay. Murine macrophage cell line RAW264.7 cells were cultured in RPMI 1640 containing 10% heat-inactivated fetal bovine serum. For assays, cells were transferred to and cultured in a 96-well black culture plate (2×10^4 cells/well) for 24 h at 37 °C, 5% CO_2. The next day, they were washed twice with cold phosphate-buffered saline (PBS) and activated with IFN-γ (100 IU/mL) and LPS (1 μg/mL) in the presence or absence of various inhibitor concentrations. Phagocytosis was assessed by measuring the amount of uptake of latex beads coated with FITC-labeled rabbit IgG into cells using a phagocytosis assay kit (FITC) (Cayman Chemical, Ann Arbor, MI) according to the instruction manual. In brief, cells with or without various stimulants were treated with the beads and cultured in RPMI 1640 without FBS (1% FBS) for 24 h at 37 °C, 5% CO_2. Twenty-four hours after stimulation, cells were washed twice with cold phosphate-buffered saline (PBS). The uptake of the beads into cells was calculated by measuring fluorescence intensity in a TECAN infinite M200 microplate fluorescence reader using an excitation of 485 nm and an emission of 535 nm. The cell supernatant from treated cells was used for measuring aminopeptidase activity. The enzymatic activity of ERAP1 was determined with L-leucine-7-amido-4-methyl coumarin (L-AMC; Sigma). The reaction mixture containing 100 μM Leu-AMC and 50 μL of culture medium in 50 mM HEPES pH 7.0, 100 mM NaCl. The amount of 7-amino-4-methylcoumarin released was measured by a TECAN infinite M200 microplate fluorescence reader at an excitation wavelength of 380 nm and an emission wavelength of 460 nm. For calculation of the ED_{50} values, experimental data were fit to the equation described in the Enzymatic Assay section using the GraphPad Prism software.

Mice. Previously described IRAP knockout mice on an Sv129 background obtained from S. Keller were backcrossed up to 10 times to C57BL/6 mice obtained from Janvier (St. Quentin-Fallavier, France). Control mice were mixed-background mice bred in our facility. RAG1-deficient OT-1 T cell receptor transgenic mice were obtained from Taconic (Germantown, NY) and bred in our animal facility. Animal experimentation was approved by the Comité d'éthique pour l'expérimentation animale Paris Descartes (no. P2.LS.156.10).

In Vitro Cross-Presentation Assays. Murine BMDCs were generated in vitro by culturing progenitor cells extruded from large bones for 7 days in complete medium (IMDM medium completed with 10% FCS, 2 mM glutamine, 100 IU/mL penicillin, 100 μg/mL streptomycin, 50 mM β-mercaptoethanol) supplemented with J558 supernatant containing 20 μg/mL GM-CSF. On day 6, BMDCs were seeded at 50 000 cells/well into a 96-well flat bottom culture plate with increasing concentrations of inhibitor **4u**. On day 7, cells were washed twice with PBS and incubated with serial dilutions of yeast cells expressing ovalbumin on their cell surface in complete medium (prepared as described in ref 39), in the presence of the same concentration of **4u** as that used before. After 6 h, the cells were washed twice with PBS, and $CD8^+$ T cells purified from lymph nodes of OT-I mice were added to the culture for 20 h at a ratio T/BMDCs of 1.5:1, again in the presence of inhibitor **4u**. To assess T cell activation, the IL-2 concentration in supernatants was measured by sandwich ELISA using Nunc Maxisorp plates, streptavidin/horse radish peroxidase (Thermo Scientific), and OptEIA TMB substrate (BD Biosciences). As negative controls, an aliquot of BMDCs were fixed with 0.04% glutaraldehyde (as described in ref 39) prior to the addition of antigen, and the signal obtained was set as the background and subtracted from all OD values. Results represent the means of duplicate wells.

Computational Methods. The crystallographic structures of ERAP1 (PDB ID: 2YD0),[40] ERAP2 (PDB ID: 3SE6),[24] and IRAP (PDB ID: 4PJ6)[41] were used without any further refinement. Polar hydrogen atoms were added and Gasteiger charges were applied using AutoDock Tools 1.5.6.[42] The initial conformations of the inhibitors were generated from SMILES representations using the program Omega 2.4,[43] and then Gasteiger charges were applied. The search space was defined by a grid box centered next to the catalytic zinc and comprised 81 × 81 × 81 grid points of 0.375 Å spacing. For each

DOI: 10.1021/jm501867s
J. Med. Chem. 2015, 58, 1524−1543

complex, 100 docking rounds were calculated with AutoDock 4.2 using the Lamarckian genetic algorithm with the default parameters of AutoDock 3.[44] The maximum number of energy evaluations was set to 10×10^6, and the docked conformations were clustered using a tolerance of 2.0 Å. Visual examination of the complexes and rendering of the figures were performed with VMD 1.9.[45] Calculations were carried out using Intel Xeon workstations running Linux 2.6.32 kernels.

■ ASSOCIATED CONTENT

Supporting Information

^{1}H and ^{13}C NMR spectra of biologically active compounds **4a**, **4u**, **4x**, and **10n**; titration curve of **4u** with recombinant mouse IRAP. This material is available free of charge via the Internet at http://pubs.acs.org.

■ AUTHOR INFORMATION

Corresponding Authors

*(D.V.) E-mail: vourloumis@chem.demokritos.gr. Phone: (+30)2106503624. Fax: (+30)2106511766.

*(E.S.) E-mail: stratos@rrp.demokritos.gr. Phone: (+30) 2106503918. Fax: (+30)2106503918.

Author Contributions

A.P. performed the computational design, synthesis, and characterization of the compounds; E.Z. prepared the recombinant enzymes and performed the in vitro and phagocytosis assays measurements and HPLC analysis; S.T. assisted in the synthesis of the compounds; F.-X.M. and P.v.E. designed and performed the cross-presentation assay; G.S and D.C.M. helped to establish the macrophage activation assay; E.A.T. co-supervised the project along with D.V. and E.S., who conceived the experiments and analyzed the results. All authors contributed to the preparation of the manuscript and have approved its final version.

Notes

The authors declare no competing financial interest.

■ ACKNOWLEDGMENTS

This research was financed by the European Union (European Social Fund) and Greek national funds through the Operational Program "Education and Lifelong Learning" of the National Strategic Reference Framework: Research Funding Program of the General Secretariat for Research & Technology (grant nos. LS7-2199 and ERC-14). F.-X.M. was supported by a grant from INSERM (poste d'accueil). Work in the laboratory of P.v.E. was supported by the Fondation pour la Recherche Médicale (grant no. DEQ20130326539).

■ ABBREVIATIONS USED

DABA, 3,4-diaminobenzoic acid; hPhe, L-homophenylalanine; hTyr, L-homotyrosine; Nle, L-norleucine; TFA, trifluoroacetic acid; HBTU, *N*,*N*,*N*′,*N*′-tetramethyl-*O*-(1*H*-benzotriazol-1-yl)-uronium hexafluorophosphate; HATU, 1-[bis(dimethylamino)-methylene]-1*H*-1,2,3-triazolo[4,5-*b*]pyridinium 3-oxid hexafluorophosphate; DIEA, *N*,*N*-diisopropylethylamine; DBU, 1,8-diazabicyclo[5.4.0]undec-7-ene; DMF, *N*,*N*-dimethylformamide

■ REFERENCES

(1) Tsujimoto, M.; Hattori, A. The oxytocinase subfamily of M1 aminopeptidases. *Biochim. Biophys. Acta* **2005**, *1751*, 9−18.

(2) Evnouchidou, I.; Papakyriakou, A.; Stratikos, E. A new role for Zn(II) aminopeptidases: antigenic peptide generation and destruction. *Curr. Pharm. Des.* **2009**, *15*, 3656−3670.

(3) Serwold, T.; Gonzalez, F.; Kim, J.; Jacob, R.; Shastri, N. ERAAP customizes peptides for MHC class I molecules in the endoplasmic reticulum. *Nature* **2002**, *419*, 480−3.

(4) Saveanu, L.; Carroll, O.; Lindo, V.; Del Val, M.; Lopez, D.; Lepelletier, Y.; Greer, F.; Schomburg, L.; Fruci, D.; Niedermann, G.; van Endert, P. M. Concerted peptide trimming by human ERAP1 and ERAP2 aminopeptidase complexes in the endoplasmic reticulum. *Nat. Immunol.* **2005**, *6*, 689−97.

(5) Weimershaus, M.; Evnouchidou, I.; Saveanu, L.; van Endert, P. Peptidases trimming MHC class I ligands. *Curr. Opin Immunol.* **2013**, *25*, 90−6.

(6) Saveanu, L.; Carroll, O.; Weimershaus, M.; Guermonprez, P.; Firat, E.; Lindo, V.; Greer, F.; Davoust, J.; Kratzer, R.; Keller, S. R.; Niedermann, G.; van Endert, P. IRAP identifies an endosomal compartment required for MHC class I cross-presentation. *Science* **2009**, *325*, 213−7.

(7) Segura, E.; Albiston, A. L.; Wicks, I. P.; Chai, S. Y.; Villadangos, J. A. Different cross-presentation pathways in steady-state and inflammatory dendritic cells. *Proc. Natl. Acad. Sci. U.S.A.* **2009**, *106*, 20377−81.

(8) Cifaldi, L.; Romania, P.; Lorenzi, S.; Locatelli, F.; Fruci, D. Role of endoplasmic reticulum aminopeptidases in health and disease: from infection to cancer. *Int. J. Mol. Sci.* **2012**, *13*, 8338−52.

(9) Alvarez-Navarro, C.; Lopez de Castro, J. A. ERAP1 structure, function and pathogenetic role in ankylosing spondylitis and other MHC-associated diseases. *Mol. Immunol.* **2014**, *57*, 12−21.

(10) Goto, Y.; Ogawa, K.; Nakamura, T. J.; Hattori, A.; Tsujimoto, M. TLR-mediated secretion of endoplasmic reticulum aminopeptidase 1 from macrophages. *J. Immunol.* **2014**, *192*, 4443−52.

(11) Goto, Y.; Ogawa, K.; Hattori, A.; Tsujimoto, M. Secretion of endoplasmic reticulum aminopeptidase 1 is involved in the activation of macrophages induced by lipopolysaccharide and interferon-gamma. *J. Biol. Chem.* **2011**, *286*, 21906−14.

(12) Aldhamen, Y. A.; Seregin, S. S.; Rastall, D. P.; Aylsworth, C. F.; Pepelyayeva, Y.; Busuito, C. J.; Godbehere-Roosa, S.; Kim, S.; Amalfitano, A. Endoplasmic reticulum aminopeptidase-1 functions regulate key aspects of the innate immune response. *PLoS One* **2013**, *8*, e69539.

(13) Aldhamen, Y. A.; Pepelyayeva, Y.; Rastall, D. P. W.; Seregin, S. S.; Zervoudi, E.; Koumantou, D.; Aylsworth, C. F.; Quiroga, D.; Godbehere, S.; Georgiadis, D.; Stratikos, E.; Amalfitano, A. Auto-immune disease-associated variants of extracellular endoplasmic reticulum aminopeptidase 1 induce altered innate immune responses by human immune cells. *J. Innate Immun.* **2015**, Jan 14. DOI:10.1159/000368899.

(14) Stratikos, E. Regulating adaptive immune responses using small molecule modulators of aminopeptidases that process antigenic peptides. *Curr. Opin. Chem. Biol.* **2014**, *23C*, 1−7.

(15) York, I. A.; Brehm, M. A.; Zendzian, S.; Towne, C. F.; Rock, K. L. Endoplasmic reticulum aminopeptidase 1 (ERAP1) trims MHC class I-presented peptides in vivo and plays an important role in immunodominance. *Proc. Natl. Acad. Sci. U.S.A.* **2006**, *103*, 9202−7.

(16) Hammer, G. E.; Gonzalez, F.; James, E.; Nolla, H.; Shastri, N. In the absence of aminopeptidase ERAAP, MHC class I molecules present many unstable and highly immunogenic peptides. *Nat. Immunol.* **2007**, *8*, 101−8.

(17) Rastall, D. P.; Aldhamen, Y. A.; Seregin, S. S.; Godbehere, S.; Amalfitano, A. ERAP1 functions override the intrinsic selection of specific antigens as immunodominant peptides, thereby altering the potency of antigen-specific cytolytic and effector memory T-cell responses. *Int. Immunol.* **2014**, *26*, 685−95.

(18) Cifaldi, L.; Lo Monaco, E.; Forloni, M.; Giorda, E.; Lorenzi, S.; Petrini, S.; Tremante, E.; Pende, D.; Locatelli, F.; Giacomini, P.; Fruci, D. Natural killer cells efficiently reject lymphoma silenced for the endoplasmic reticulum aminopeptidase associated with antigen processing. *Cancer Res.* **2011**, *71*, 1597−606.

DOI: 10.1021/jm501867s
J. Med. Chem. 2015, 58, 1524−1543

(19) James, E.; Bailey, I.; Sugiyarto, G.; Elliott, T. Induction of protective antitumor immunity through attenuation of ERAAP function. *J. Immunol.* **2013**, *190*, 5839−46.
(20) Nagarajan, N. A.; Gonzalez, F.; Shastri, N. Nonclassical MHC class Ib-restricted cytotoxic T cells monitor antigen processing in the endoplasmic reticulum. *Nat. Immunol.* **2012**, *13*, 579−86.
(21) Zervoudi, E.; Saridakis, E.; Birtley, J. R.; Seregin, S. S.; Reeves, E.; Kokkala, P.; Aldhamen, Y. A.; Amalfitano, A.; Mavridis, I. M.; James, E.; Georgiadis, D.; Stratikos, E. Rationally designed inhibitor targeting antigen-trimming aminopeptidases enhances antigen presentation and cytotoxic T-cell responses. *Proc. Natl. Acad. Sci. U.S.A.* **2013**, *110*, 19890−5.
(22) Chen, L.; Fischer, R.; Peng, Y.; Reeves, E.; McHugh, K.; Ternette, N.; Hanke, T.; Dong, T.; Elliott, T.; Shastri, N.; Kollnberger, S.; James, E.; Kessler, B.; Bowness, P. Critical role of endoplasmic reticulum aminopeptidase 1 in determining the length and sequence of peptides bound and presented by HLA-B27. *Arthritis Rheumatol.* **2014**, *66*, 284−94.
(23) Papakyriakou, A.; Zervoudi, E.; Theodorakis, E. A.; Saveanu, L.; Stratikos, E.; Vourloumis, D. Novel selective inhibitors of aminopeptidases that generate antigenic peptides. *Bioorg. Med. Chem. Lett.* **2013**, *23*, 4832−6.
(24) Zervoudi, E.; Papakyriakou, A.; Georgiadou, D.; Evnouchidou, I.; Gajda, A.; Poreba, M.; Salvesen, G. S.; Drag, M.; Hattori, A.; Swevers, L.; Vourloumis, D.; Stratikos, E. Probing the S1 specificity pocket of the aminopeptidases that generate antigenic peptides. *Biochem. J.* **2011**, *435*, 411−20.
(25) Stratikos, E.; Stern, L. J. Antigenic peptide trimming by ER aminopeptidases—insights from structural studies. *Mol. Immunol.* **2013**, *55*, 212−9.
(26) Birtley, J. R.; Saridakis, E.; Stratikos, E.; Mavridis, I. M. The crystal structure of human endoplasmic reticulum aminopeptidase 2 reveals the atomic basis for distinct roles in antigen processing. *Biochemistry* **2012**, *51*, 286−295.
(27) Nguyen, T. T.; Chang, S. C.; Evnouchidou, I.; York, I. A.; Zikos, C.; Rock, K. L.; Goldberg, A. L.; Stratikos, E.; Stern, L. J. Structural basis for antigenic peptide precursor processing by the endoplasmic reticulum aminopeptidase ERAP1. *Nat. Struct. Mol. Biol.* **2011**, *18*, 604−13.
(28) Lukaszuk, A.; Demaegdt, H.; Szemenyei, E.; Toth, G.; Tymecka, D.; Misicka, A.; Karoyan, P.; Vanderheyden, P.; Vauquelin, G.; Tourwe, D. Beta-homo-amino acid scan of angiotensin IV. *J. Med. Chem.* **2008**, *51*, 2291−6.
(29) Andersson, H.; Demaegdt, H.; Vauquelin, G.; Lindeberg, G.; Karlen, A.; Hallberg, M.; Erdelyi, M.; Hallberg, A. Disulfide cyclized tripeptide analogues of angiotensin IV as potent and selective inhibitors of insulin-regulated aminopeptidase (IRAP). *J. Med. Chem.* **2010**, *53*, 8059−71.
(30) Andersson, H.; Demaegdt, H.; Johnsson, A.; Vauquelin, G.; Lindeberg, G.; Hallberg, M.; Erdelyi, M.; Karlen, A.; Hallberg, A. Potent macrocyclic inhibitors of insulin-regulated aminopeptidase (IRAP) by olefin ring-closing metathesis. *J. Med. Chem.* **2011**, *54*, 3779−92.
(31) Albiston, A. L.; Morton, C. J.; Ng, H. L.; Pham, V.; Yeatman, H. R.; Ye, S.; Fernando, R. N.; De Bundel, D.; Ascher, D. B.; Mendelsohn, F. A.; Parker, M. W.; Chai, S. Y. Identification and characterization of a new cognitive enhancer based on inhibition of insulin-regulated aminopeptidase. *FASEB J.* **2008**, *22*, 4209−17.
(32) Mountford, S. J.; Albiston, A. L.; Charman, W. N.; Ng, L.; Holien, J. K.; Parker, M. W.; Nicolazzo, J. A.; Thompson, P. E.; Chai, S. Y. Synthesis, structure-activity relationships and brain uptake of a novel series of benzopyran inhibitors of insulin-regulated aminopeptidase. *J. Med. Chem.* **2014**, *57*, 1368−77.
(33) Borhade, S. R.; Rosenström, U.; Sävmarker, J.; Lundbäck, T.; Jenmalm-Jensen, A.; Sigmundsson, K.; Axelsson, H.; Svensson, F.; Konda, V.; Sköld, C.; Larhed, M.; Hallberg, M. . Inhibition of insulin-regulated aminopeptidase (IRAP) by arylsulfonamides. *ChemistryOpen* **2014**, *3*, 256−263.
(34) Kuiper, J. J.; Van Setten, J.; Ripke, S.; Van' t Slot, R.; Mulder, F.; Missotten, T.; Baarsma, G. S.; Francioli, L. C.; Pulit, S. L.; De Kovel, C. G.; Ten Dam-Van Loon, N.; Den Hollander, A. I.; Veld, P. H.; Hoyng, C. B.; Cordero-Coma, M.; Martin, J.; Llorenc, V.; Arya, B.; Thomas, D.; Bakker, S. C.; Ophoff, R. A.; Rothova, A.; De Bakker, P. I.; Mutis, T.; Koeleman, B. P. A genome-wide association study identifies a functional ERAP2 haplotype associated with birdshot chorioretinopathy. *Hum. Mol. Genet.* **2014**, *23*, 6081−7.
(35) Fruci, D.; Ferracuti, S.; Limongi, M. Z.; Cunsolo, V.; Giorda, E.; Fraioli, R.; Sibilio, L.; Carroll, O.; Hattori, A.; van Endert, P. M.; Giacomini, P. Expression of endoplasmic reticulum aminopeptidases in EBV-B cell lines from healthy donors and in leukemia/lymphoma, carcinoma, and melanoma cell lines. *J. Immunol.* **2006**, *176*, 4869−79.
(36) Albiston, A. L.; Diwakarla, S.; Fernando, R. N.; Mountford, S. J.; Yeatman, H. R.; Morgan, B.; Pham, V.; Holien, J. K.; Parker, M. W.; Thompson, P. E.; Chai, S. Y. Identification and development of specific inhibitors for insulin-regulated aminopeptidase as a new class of cognitive enhancers. *Br. J. Pharmacol.* **2011**, *164*, 37−47.
(37) Gerritz, S. W.; Sefler, A. M. 2,5-Dimethylfuran (DMFu): an internal standard for the "traceless" quantitation of unknown samples via ^{1}H NMR. *J. Comb. Chem.* **2000**, *2*, 39−41.
(38) Jahani, F.; Tajbakhsh, M.; Golchoubian, H.; Khaksar, S. Guanidine hydrochloride as an organocatalyst for N-Boc protection of amino groups. *Tetrahedron Lett.* **2011**, *52*, 1260−1264.
(39) Saveanu, L.; van Endert, P. Preparing antigens suitable for cross-presentation assays in vitro and in vivo. *Methods Mol. Biol.* **2013**, *960*, 389−400.
(40) Kochan, G.; Krojer, T.; Harvey, D.; Fischer, R.; Chen, L.; Vollmar, M.; von Delft, F.; Kavanagh, K. L.; Brown, M. A.; Bowness, P.; Wordsworth, P.; Kessler, B. M.; Oppermann, U. Crystal structures of the endoplasmic reticulum aminopeptidase-1 (ERAP1) reveal the molecular basis for N-terminal peptide trimming. *Proc. Natl. Acad. Sci. U.S.A.* **2011**, *108*, 7745−50.
(41) Hermans, S. J.; Ascher, D. B.; Hancock, N. C.; Holien, J. K.; Michell, B. J.; Yeen Chai, S.; Morton, C. J.; Parker, M. W. Crystal structure of human insulin-regulated aminopeptidase with specificity for cyclic peptides. *Protein Sci.* **2014**, *24*, 190−9.
(42) Morris, G. M.; Huey, R.; Lindstrom, W.; Sanner, M. F.; Belew, R. K.; Goodsell, D. S.; Olson, A. J. AutoDock4 and AutoDockTools4: automated docking with selective receptor flexibility. *J. Comput. Chem.* **2009**, *30*, 2785−91.
(43) Hawkins, P. C.; Skillman, A. G.; Warren, G. L.; Ellingson, B. A.; Stahl, M. T. Conformer generation with OMEGA: algorithm and validation using high quality structures from the Protein Databank and Cambridge Structural Database. *J. Chem. Inf. Model.* **2010**, *50*, 572−84.
(44) Huey, R.; Morris, G. M.; Olson, A. J.; Goodsell, D. S. A semiempirical free energy force field with charge-based desolvation. *J. Comput. Chem.* **2007**, *28*, 1145−1152.
(45) Humphrey, W.; Dalke, A.; Schulten, K. VMD: visual molecular dynamics. *J. Mol. Graphics* **1996**, *14*, 33−8.

DOI: 10.1021/jm501867s
J. Med. Chem. 2015, 58, 1524−1543